CHAPTER 6
Numerical Modelling

6.1 Introduction

In this chapter, finite element (FE) models developed to simulate the flexural behavior of the masonry beams strengthened with ECC sheet (included in Chapter 4) and ECC strengthened masonry walls with and without opening (included in Chapter 5) are presented. The main aims of conducting finite element analyses were (i) to evaluate the effect of ECC sheet on the flexural response of masonry beams and walls (ii) to identify the parametric study on ECC strengthened masonry beams and walls because all the experimental programs are not possible in real life; and (iii) to provide a design chart which is useful for determining the necessary ECC reinforcement ratio as per required strength. A commercial finite element software package, ABAQUS (Dassault Systemes) was used in this research programme. This chapter has been discussed in three sections.

The first section deals with the numerical modelling approach for the masonry and ECC. The suitable material model for masonry and ECC available in the ABAQUS is described. The bonding materials such as epoxy and cement mortar are modelled as the cohesive elements. The experimentally obtained material properties of masonry and ECC sheets were used in the numerical modeling.

The second section deals with the numerical modelling of the flexural response of burnt-clay brick masonry beams externally strengthened using precast ECC sheet on tension face and/ or both on tension as well as compression face of masonry beams. Detailed parametric study has been performed which incorporates the effect of various parameters such as ECC thickness in compression and tension, epoxy, and cement mortar as bonding agents, and bonding agent thickness on the flexural response of strengthened beams.

The third section deals with the numerical modelling of ECC strengthened masonry walls with and without opening. ECC sheets were bonded to masonry walls using epoxy adhesive. The influence of mesh size on the numerical results are also reported. A parametric study has been carried out to examine the effect of various parameters such as ECC reinforcement ratios, width to thickness ratios, and span length to depth ratios of masonry walls.

6.2 Numerical Modelling

Masonry is a composite material, consisting of masonry units and mortar joints in both the horizontal and vertical directions. Therefore, modelling of masonry is more complex than modelling of comparatively homogeneous construction materials such as steel and concrete, because the behavior of masonry is dependent upon both orientation of masonry constituents and its strength [153]. There are mainly three approaches to simulate the nonlinear behavior of masonry structures depending on the degree of accuracy and simplicity desired [154] as follow:

i. *Detailed micro-modelling*: In this approach, masonry units and mortar are represented by continuum elements whereas brick-mortar interface is represented by discontinuous elements.
ii. *Simplified micro-modelling*: In this method, masonry units are represented by continuum elements whereas the behavior of the mortar joints and brick-mortar interface is lumped in discontinuous elements.
iii. *Macro-modelling:* The macro modelling approach does not make a distinction between individual brick units and mortar joints but treats masonry as a homogeneous model.

The first two approaches are most accurate model for describing masonry behavior but these require a large computation memory and huge time for the analysis of masonry structures. The last approach (macro-modelling) gives a better understanding about the global behavior of masonry structure, where the interaction between brick and mortar are generally negligible [118]. This approach is best to study the behavior of large masonry walls, where few experimental tests are sufficient for calibrating the material properties. In this study, macro-modelling was done by considering the masonry as composite homogeneous model. The critical feature of the homogeneous model is that the strong mortar, weak brick, and brick-mortar interfaces are smeared so that the entire masonry is represented by a homogeneous isotropic material. The graphical user interface i.e., ABAQUS CAE was used to create all the parts, models, define boundary conditions, apply loads, submit jobs, monitor the analysis, and evaluate the results. Solid elements C3D8R, i.e. linear 8 nodes isoparametric three-dimensional brick elements with reduced integration were used for masonry and ECC sheet. The element type COH3D8, i.e. 8 nodes three-dimensional cohesive element was used for epoxy and cement mortar.

6.2.1 Material model

ABAQUS does not include any specific model for modelling the masonry behavior, and consequently, the behavior of masonry was considered here similar to that of concrete, because both materials are strong in compression and weak in tension. Masonry is, however, does not have homogeneous properties similar to concrete but it is considered to be homogeneous here for simplicity. The concrete-damaged plasticity (CDP) model is a continuum plasticity based damage model for simulation of constitutive behavior of concrete. This model was theoretically described by Lubliner et al. [155] and developed by Lee and Fenves [156]. It provides a general capability for modelling concrete and other quasi-brittle materials in all types of structures. ABAQUS uses the concept of isotropic damage in combination with isotropic tensile and compression plasticity in order to represent the inelastic behavior of material [157]. The key aspects of CDP model in ABAQUS include the yield criterion, hardening rule, softening rule, flow rule, the compressive and tensile behavior along with damage variables. The CDP parameters were used to model the masonry and ECC sheet as they precisely account the nonlinear material behavior. These nonlinear material properties reflect the material behavior beyond elastic range. It assumes that the failure of masonry and ECC can be modeled using the plasticity characteristics and response to uniaxial compression and uniaxial tension.

Plasticity parameter: The plasticity parameters of masonry and ECC used for this study are presented in Table 6.1. The dilation angle (ψ) measured in the p-q plane at high confining pressure is determined with sensitivity analysis. The flow potential eccentricity (ε), which defines the rate at which the hyperbolic flow potential approaches its asymptote and default value of 0.1 is taken. Another parameter describing the state of the materials is the point at which the concrete undergoes failure under biaxial compression. The f_{bo}/f_{co} is a ratio of the initial biaxial compressive yield stress to initial uniaxial compressive yield stress. The most reliable in this regard are the experimental results reported by Kupfer et al. [158]. The ABAQUS user's manual [157] specifies default value of f_{bo}/f_{co} as 1.16. K_c is the ratio of the second stress invariant on the tensile meridian to that on the compressive meridian at initial yield for any given value of the pressure invariant such that the maximum principal stress is negative and it must satisfy the condition of $0.5 < Kc \leq 1$. The default value of 0.667 for K_c is used in this study. Material models exhibiting softening behavior and stiffness degradation often lead to severe convergence difficulties in implicit analysis programs. Viscoplastic regularization is used to overcome some of these convergence difficulties which

cause the consistent tangent stiffness of the softening material to become positive for sufficiently small-time increments. The viscoplastic regularization technique will permit stresses to be outside of the yield surface. The small value of viscoplastic regularization usually helps improve the rate of convergence of the model in the softening regime, without compromising results. The viscosity parameter is taken as 1×10^{-5} after many sensitivity analyses that were performed.

Table 6.1 Plasticity parameters used for CDP model for masonry and ECC

Type of material	Dilation angle, (ψ)	Eccentricity, (ε)	f_{bo}/f_{co}	K_c	Viscosity parameters, (μ_v)
Masonry	30°	0.1	1.16	0.667	1×10^{-5}
ECC	37°	0.1	1.16	0.667	1×10^{-5}

Compressive behavior: The compressive stress-strain relationship with damage properties when it is subjected to uniaxial loading is shown in Fig. 6.1. The response is linear until the initial value of yield stress (σ_{co}) is reached (Point A). In the plastic regime, the response is typically characterized by stress hardening followed by strain softening. Compressive yield stress (σ_c) values are provided in ABAQUS as a tabular function of inelastic or crushing strain ($\tilde{\varepsilon}_c^{in}$). The compressive hardening data are provided in terms of inelastic strain ($\tilde{\varepsilon}_c^{in}$), which is determined as the difference between the total strain and the elastic strain that corresponds to undamaged material as provided in Eq. 6.1.

$$\tilde{\varepsilon}_c^{in} = \varepsilon_c - \varepsilon_{oc}^{el} \tag{6.1}$$

where, $\varepsilon_{oc}^{el} = \frac{\sigma_c}{E_o}$, ε_{oc}^{el} = Elastic strain corresponding to the undamaged material and ε_c = total compressive strain. For example, in Fig. 6.1, at point C, if total stress = σ_{cc}, the corresponding strain = ε_{cc}, from Eq. 6.1, inelastic strain at point C $\left(\tilde{\varepsilon}_{cc}^{in}\right)$ equals to total strain at point C (ε_{cc}) minus the elastic strain at point C $\left(\varepsilon_{oc}^{el} = \frac{\sigma_{cc}}{E_o}\right)$. Similarly, inelastic strain corresponding to respective yield stress is calculated on different intervals of compressive stress-strain response. Further, plastic strains calculated using Eq.6. 2 are neither negative nor decreasing with increased stresses [157].

$$\tilde{\varepsilon}_c^{pl} = \tilde{\varepsilon}_c^{in} - \frac{d_c}{(1-d_c)}\frac{\sigma_c}{E_o} \tag{6.2}$$

where, d_c is referred to uniaxial damage variables for compression. The compressive damage variable (d_c) is the rate of degradation of the material stiffness which holds true for region beyond peak compressive stress (Point B in Fig. 6.1) and calculated using Eq. 6.3.

$$d_c = \begin{cases} 0, \\ 1-\dfrac{\sigma_c}{\sigma_{cu}}, \quad after\ peak\ stress \end{cases} \tag{6.3}$$

where, σ_{cu} is peak compressive yield stress.

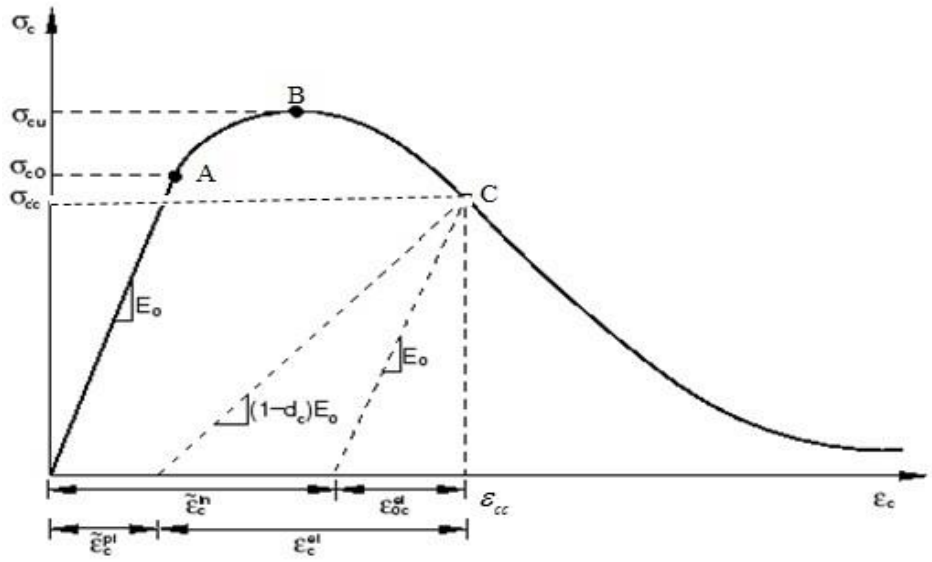

Fig. 6.1 Uniaxial compressive stress-strain relationship [157]

Tensile behavior: In order to simulate the complete tensile stress-strain behavior in ABAQUS, a post failure stress-strain relationship is shown in Fig. 6.2. The uniaxial stress-strain response is assumed linear elastic up to its tensile stress (Point A). After cracking, the descending trend is modeled by a softening process as in terms of cracking strain. The cracking strain $\left(\tilde{\varepsilon}_t^{ck}\right)$ is calculated by ABAQUS as the difference between the total strain and the elastic strain that corresponds to the undamaged material as given in Eq. 6.4.

$$\tilde{\varepsilon}_t^{ck} = \varepsilon_t - \varepsilon_{ot}^{el} \tag{6.4}$$

where, $\varepsilon_{ot}^{el} = \frac{\sigma_t}{E_o}$, ε_{ot}^{el} = Elastic strain corresponding to the undamaged material and ε_t = total tensile strain. Further, plastic strains calculated using Eq. 6.5 are neither negative nor decreasing with increased stresses [157].

$$\tilde{\varepsilon}_t^{pl} = \tilde{\varepsilon}_t^{cr} - \frac{d_t}{(1-d_t)}\frac{\sigma_t}{E_o} \tag{6.5}$$

where, d_t is referred to uniaxial damage variables for tension. The tensile damage variable (d_t) is the rate of degradation of the material stiffness which holds true for region beyond peak tensile stress (Point A in Fig. 6.2) and calculated using Eq. 6.6.

$$d_t = \begin{cases} 0, \\ 1 - \frac{\sigma_t}{\sigma_{to}}, \quad after\ peak\ stress \end{cases} \tag{6.6}$$

where, σ_{to} is peak tensile yield stress.

The material properties (yield stress versus inelastic/cracking strain) used in the numerical modelling were obtained from material characterization tests performed and are listed in Tables 6.2 & 6.3, with the exception of the following assumptions: (a) the Masonry tensile strength is taken as 10% of its measured compressive strength [118 & 57], (b) the Poisson's ratio of the masonry is assumed to be 0.2 [159]. The experimentally obtained material properties of masonry and ECC sheets were used in the numerical modelling. The modulus of elasticity of masonry and ECC used for analytical modelling are 1250 MPa, 8200 MPa, respectively.

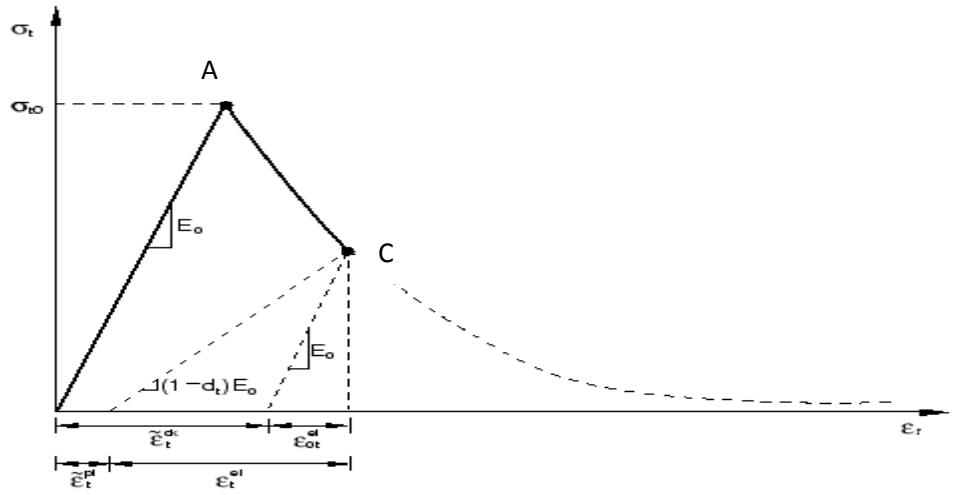

Fig. 6.2 Uniaxial tensile stress-strain relationship [157]

Table 6.2 Yield stress and corresponding strain values of masonry

Compression stiffening properties		**Tension stiffening properties**	
Yield stress (MPa)	Inelastic strain × 10^{-2}	Yield stress (MPa)	Cracking strain × 10^{-2}
1.51	0.00	0.36	0.00
2.24	0.06	0.05	0.68
3.24	0.10	-	-
3.61	0.12	-	-
3.07	0.40	-	-
2.50	0.75	-	-

Table 6.3 Yield stress and corresponding strain values of ECC

Compression stiffening properties		**Tension stiffening properties**	
Yield stress (MPa)	Inelastic strain × 10^{-2}	Yield stress (MPa)	Cracking strain × 10^{-2}
31.20	0.00	2.65	0.00
42.31	0.05	2.70	0.17
51.10	0.17	1.64	0.25
39.53	1.46	0.69	0.36
30.12	2.78	0.65	0.37
20.52	5.02	-	-

6.2.2 Cohesive behavior

ECC sheet was bonded to masonry surface using epoxy and it is considered to be a thin viscous film that provides a surface to surface contact between the masonry surface and ECC sheet. Epoxy was defined as cohesive elements and traction separation law was used. The model assumes a linear elastic traction-separation law prior to damage and the failure of cohesive bond is characterized by progressive degradation of the cohesive stiffness, derived from a damage process. ABAQUS imposes this contact behavior only for node-to-surface interactions which mean that each contact interaction needs to be assigning a slave surface to a master surface while a master surface can interact with several slave surfaces. The traction-separation model in ABAQUS assumes initially linear elastic behavior, followed by the initiation and evolution of damage. The elastic constitutive matrix that relates the normal and shear stresses to the normal and shear separations across the interface defines the model as in Eq. 6.7 [157].

$$t = \begin{Bmatrix} t_n \\ t_s \\ t_t \end{Bmatrix} = \begin{bmatrix} K_{nn} & K_{ns} & K_{nt} \\ K_{ns} & K_{ss} & K_{st} \\ K_{nt} & K_{st} & K_{tt} \end{bmatrix} \begin{Bmatrix} \delta_n \\ \delta_s \\ \delta_t \end{Bmatrix} = K\delta \tag{6.7}$$

where t is the nominal traction stress vector and δ, the corresponding separations. n stands for the normal direction while s and t stands for the in-plane principal directions (tangential and shear directions). In this study, the stiffness components in normal, shear, and tangential directions are considered to have uncoupled cohesive behavior. The off-diagonal terms in the elasticity matrix are set to zero as the normal, shear, and tangential components are uncoupled. The normal stiffness K_{nn} was determined as the ratio of the modulus of elasticity and thickness of the adhesive layer. Similarly, in the two shear directions, the shear stiffness (K_{ss} & K_{tt}) was determined as the ratio of shear modulus and the thickness.

6.3 FE Models for Masonry Beams Strengthened with ECC Sheets

This section demonstrates the numerical modelling of masonry beams strengthened with ECC sheets by bonding them on tension face as well as both on tension and compression faces like a sandwich beam. The experimental details of these beams are explained in Chapter 4 (Section 4.3). This section deals with the validation of numerical models with the experimental results and parametric study of strengthened masonry beams. Table 6.4 depicts the nomenclature and

descriptions of beams used in the study. To distinguish the tested specimens, and analytical modelled specimens, the designation ‘X-E’ and ‘X-A’ are used, where ‘X’ indicate the specimens described in Table 6.4; ‘E’ stands for experimentally tested specimen; ‘A’ refers to the numerically modelled specimen.

Table 6.4 Details of beam specimens

Sr. No.	Beam designation	Beam description*
1.	M-A, M-E	Masonry control beam of depth 110 mm
2.	ECC-A, ECC-E	ECC control beam of depth 35 mm
3.	ET-A, ET-E	Epoxy-bonded tension strengthened beam with ECC thickness 35 mm on tension face.
4.	CT-A, CT-E	Cement mortar bonded tension strengthened beam with ECC thickness 35 mm on tension face.
5.	ECT-A, ECT-E	Epoxy-bonded Sandwich beam with ECC thickness 35 mm on both faces.
6.	CCT-A, CCT-E	Cement mortar bonded Sandwich beam with ECC thickness 35 mm on both faces.
7.	35-25-ECT, 35-30-ECT, 35-40-ECT, 35-45-ECT, 35-50-ECT	Epoxy-bonded Sandwich beam with ECC thickness 35 mm on compression face and 25, 30, 40, 45, 50 mm, respectively on tension face.
8.	25-35-ECT, 30-35-ECT, 40-35-ECT, 45-35-ECT, 50-35-ECT	Epoxy-bonded Sandwich beam with ECC thickness 35 mm on tension face and 25, 30, 40, 45, 50 mm, respectively on compression face.

9.	25-ET, 30-ET, 40-ET, 45-ET, 50-ET	Epoxy-bonded tension strengthened beam with ECC thickness 25, 30, 40, 45, and 50 mm, respectively on tension face.
10.	ECT-0.5, ECT-0.8, ECT-01, ECT-02, ECT-03	Epoxy-bonded Sandwich beam using ECC sheet of thickness 35 mm on both faces (tension and compression) with Epoxy thickness 0.5, 0.8, 1, 2, and 3 mm, respectively.
11.	ET-0.5, ET-0.8, ET-01, ET-02, ET-03	Epoxy-bonded tension strengthened beam using ECC sheet of thickness 35 mm on tension face with Epoxy thickness 0.5, 0.8, 1, 2, and 3 mm, respectively.
12.	35-20-CCT, 35-25-CCT, 35-30-CCT, 35-40-CCT, 35-45-CCT	Cement mortar bonded Sandwich beam with ECC thickness 35 mm on compression face and 20, 25, 30, 40, 45 mm, respectively on tension face.
13.	20-35-CCT, 25-35-CCT, 30-35-CCT, 40-35-CCT, 45-35-CCT	Cement mortar bonded Sandwich beam with ECC thickness 35 mm on tension face and 20, 25, 30, 40, 45 mm, respectively on compression face.
14.	25-CT, 30-CT, 40-CT, 45-CT, 50-CT	Cement mortar bonded tension strengthened beam with ECC thickness 25, 30, 40, 45, and 50 mm, respectively on tension face.

15.	CCT-02, CCT-04, CCT-05, CCT-10	Cement mortar bonded Sandwich beam using ECC sheet of 35 mm thick on both faces (tension and compression) with cement mortar of thickness 2, 4, 5, and 10, respectively.
16.	CT-02, CT-04, CT-05, CT-10	Cement mortar bonded tension strengthened beam using ECC sheet of 35 mm thick with cement mortar of thickness 2 mm, 4 mm, 5 mm, and 10 mm, respectively.

*In specimen designated as X-A or X-E, 'X' refers to specimens described; 'E' stands for experimentally tested specimen; 'A' refers to the numerically modelled specimen.

6.3.1 Validation of numerical models

The details of comparison of results obtained using ABAQUS and experimental flexural response tests on control and precast ECC strengthened masonry beams (i.e., tension strengthened and sandwich beams) are presented in Table 6.5. The average load-displacement response of experimentally tested and numerical modelled specimens of control and strengthened masonry beams are shown in Figs. 6.3-6.9. In the figures and tables, notations with last letters E and A, respectively refers to experimental and numerical results. Figure 6.3 shows the comparison of flexural responses of control masonry beam obtained using ABAQUS and experimental 4-point flexural tests. It is observed that the flexural response of the control masonry beam is in close proximity to the corresponding experimental response with maximum deviation of 14.68% in the peak load and 2.02% corresponding deflections. The deformed shape of the control masonry beam is shown in Fig. 6.4. Similarly, it is shown in Fig. 6.5 that numerically and experimentally obtained flexural responses of the ECC strips of 35 mm thickness are in close agreement. Thus, it is demonstrated that the modeling of control masonry beams and ECC strips for flexural loading using ABAQUS gives satisfactory results as they are close to the corresponding experimental results. The comparison of numerical results obtained using ABAQUS for epoxy bonded sandwich beam (ECT-A) with corresponding experimental results (ECT-E) is shown in Fig. 6.6. As mentioned earlier and shown in Table 6.4, thickness of ECC strip used in beams (ECT-A & E) is 35 mm and epoxy has been used as bonding agent. It is seen that the numerical and experimental responses are close with maximum deviation of 7.56 % in peak loads. However, the stiffness of numerically modelled beam is slightly more and may be attributed to pre-cracking flexural

response not considered in the modelling. The results obtained by ABAQUS for sandwich beam with cement mortar as bonding agent (CCT-A) is validated with the corresponding experimental results (CCT-E) as shown in Fig. 6.7. It is observed from Fig. 6.7 that the numerically obtained flexural response of sandwich beam with cement mortar as bonding agent is in close agreement with the corresponding experimental results. The ABAQUS results for beam strengthened in tension with epoxy as bonding agent (ET-A) is validated with the corresponding experimental result (ET-E) and shown in Fig. 6.8. The nature of load versus deflection curve is observed to be similar. As shown in Fig. 6.8, the numerically obtained flexural response of tension strengthened beam with epoxy as bonding agent is in close proximity to experimental result with a maximum deviation of 25.97% in peak load. The validation of results obtained using ABAQUS for the beam (CT-A) strengthened in tension with cement mortar as bonding agent with the corresponding experimental result (CT-E) is shown in Fig. 6.9. The nature of load versus deflection curve is observed to be similar. It is observed that the flexural response obtained with ABAQUS is in close proximity to the corresponding experimental results with a maximum deviation of 7.69 % in peak load.

Table 6.5 Validation of experimental results with numerical study

Beam designation	Experimental		Numerical		% age error in peak load	% age error in mid-span deflection
	Peak load (kN)	Mid-span deflection (mm)	Peak load (kN)	Mid-span deflection (mm)		
M	2.18	0.99	2.50	0.97	14.68	2.02
ECC	0.65	2.66	0.64	2.07	1.54	22.18
ET	7.70	2.80	5.70	2.30	25.97	17.86
CT	3.90	2.30	4.20	2.60	7.69	13.04
ECT	11.25	2.23	10.40	2.55	7.56	14.35
CCT	9.58	2.32	9.50	2.63	0.84	13.36

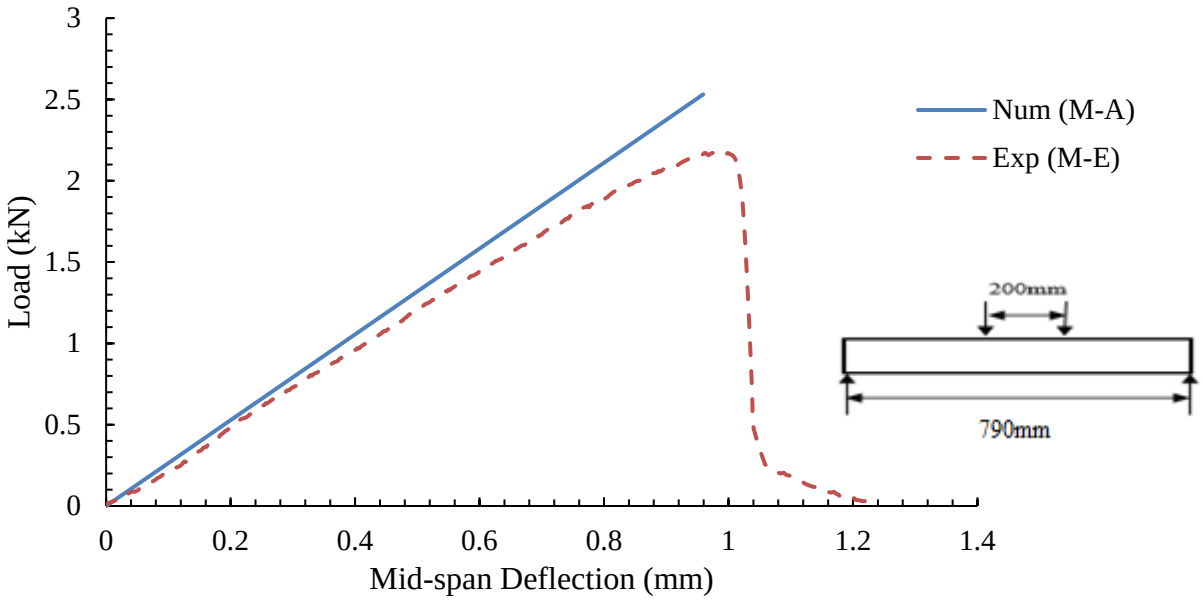

Fig. 6.3 Numerical validation of control masonry beam with experimental results

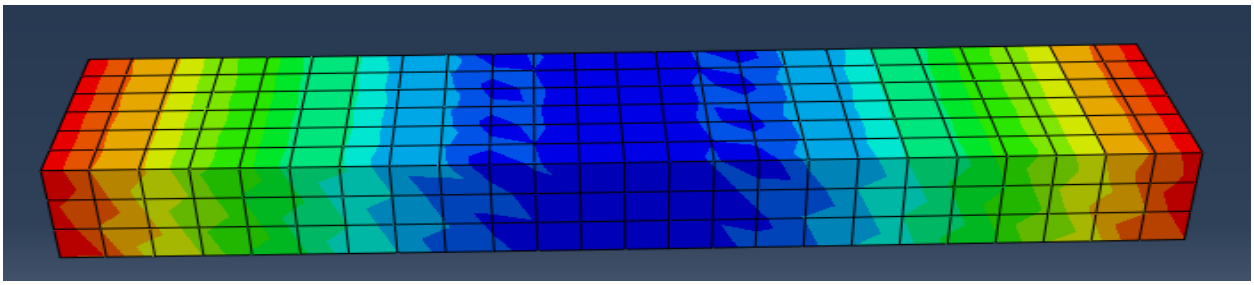

Fig. 6.4 Deformed shape of the control masonry beam (M-A)

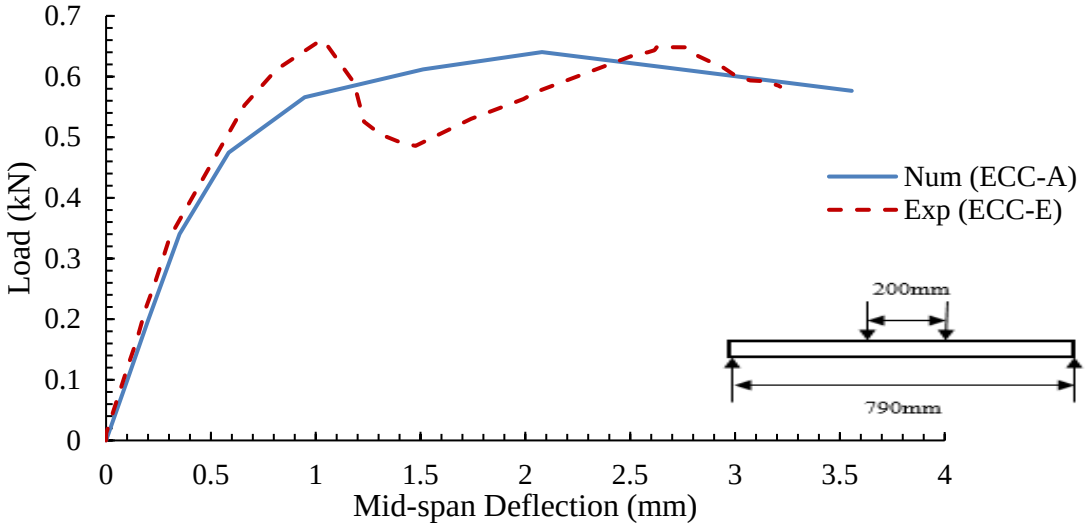

Fig.6.5 Numerical validation of control ECC beam for flexure with experimental results

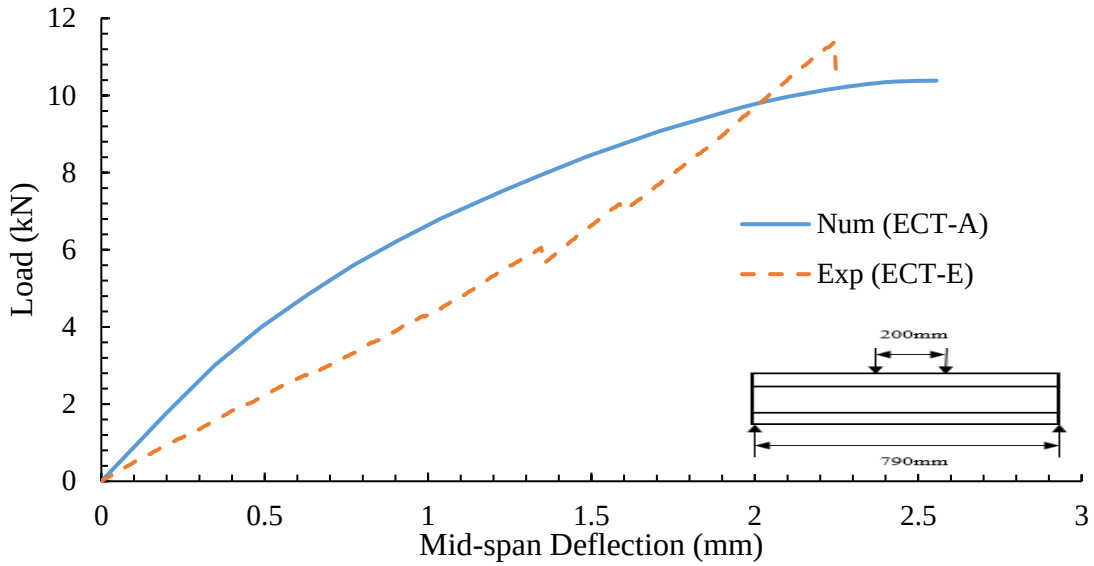

Fig. 6.6 Numerical validation of sandwich beam with epoxy as bonding agent for flexure with experimental results

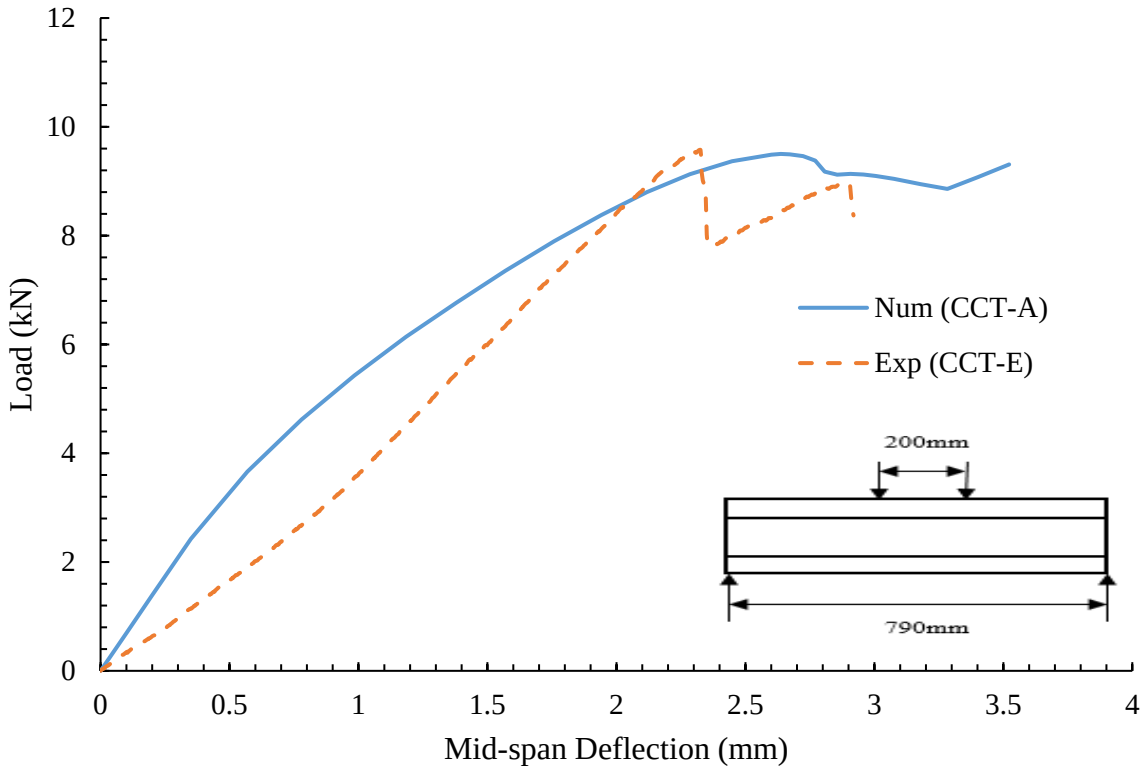

Fig. 6.7 Numerical validation of sandwich beam with cement mortar as bonding agent for flexure with experimental results

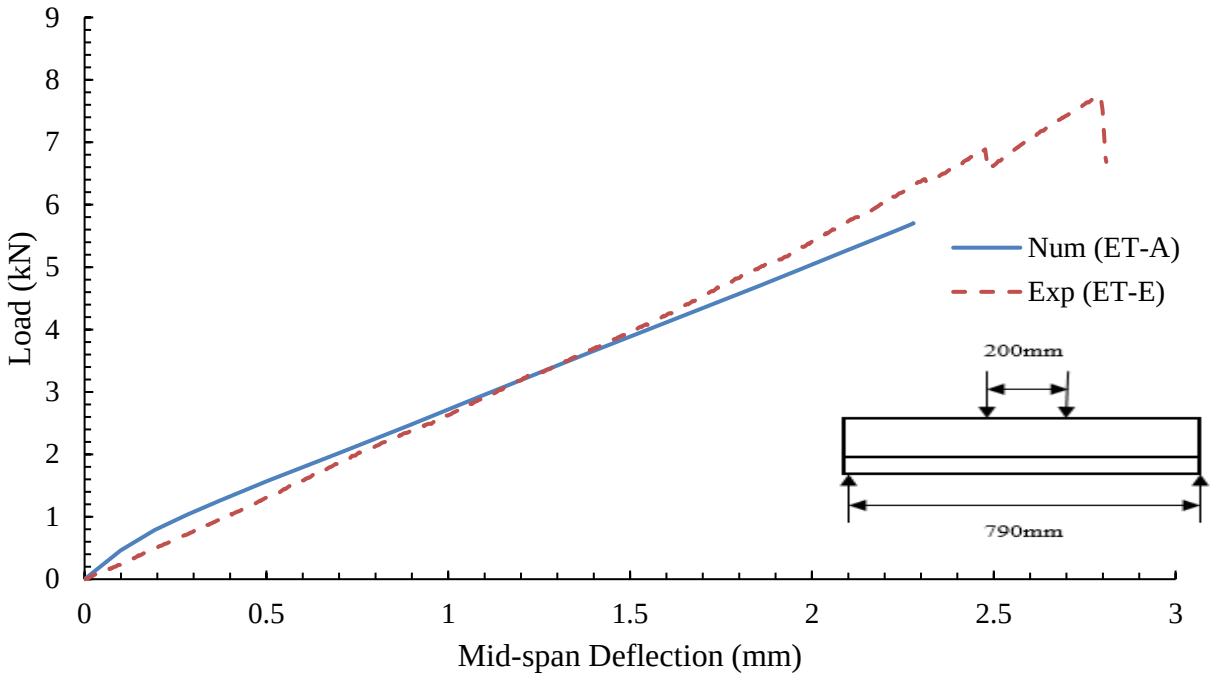

Fig. 6.8 Numerical validation of tension strengthened beam with epoxy as bonding agent for flexure with experimental results

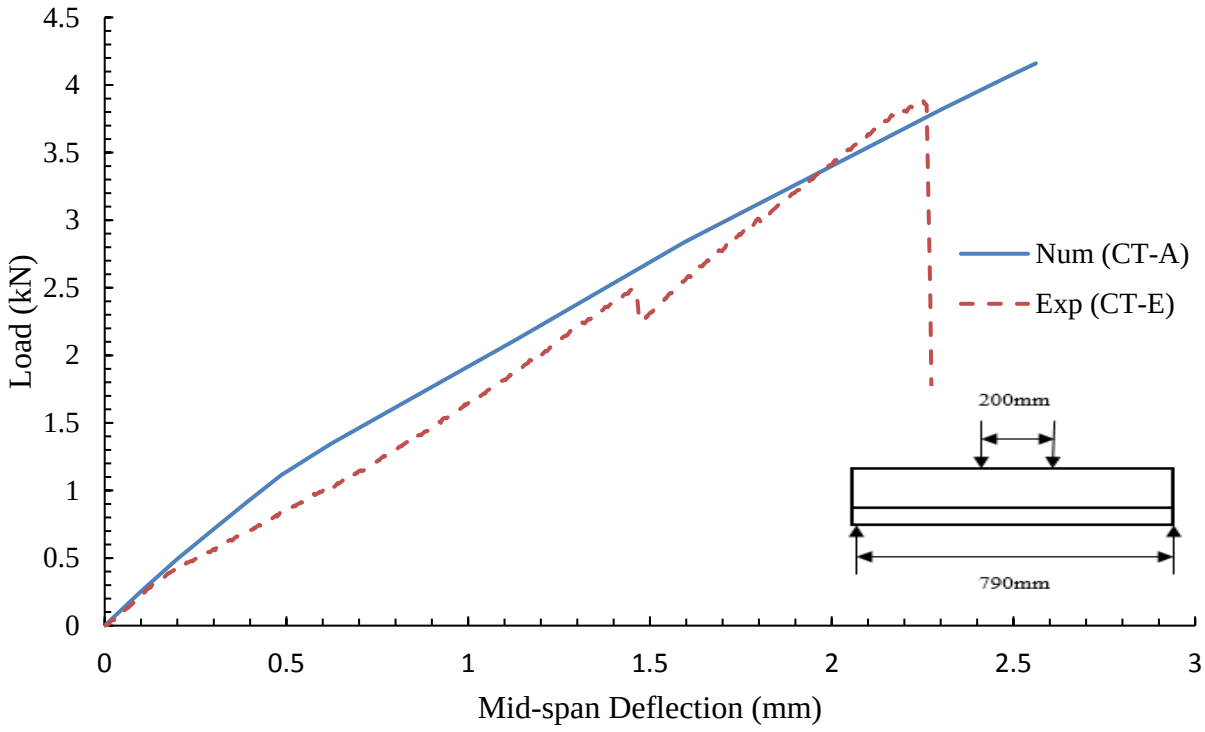

Fig. 6.9 Numerical validation of tension strengthened beam with cement mortar as bonding agent for flexure with experimental results

6.3.2 Results and discussion of parametric study

Effect of thickness of ECC strip/plate in tension on the flexural response of sandwich beams with epoxy as bonding agent is shown in Fig. 6.10, while the effect of thickness of ECC strip in tension on the flexural response of sandwich beams with cement mortar as bonding agent is shown in Fig. 6.11. Similarly, the effect of thickness of ECC strip in tension on flexural response of tension strengthened beams with epoxy as bonding agent is shown in Fig. 6.12 while the effect of thickness of ECC strip in tension on flexural response of tension strengthened beams with cement mortar as bonding agent is shown in Fig. 6.13. It may be noted that while varying the thickness of ECC strip on tension face, the compression face ECC strip thickness is kept constant as 35 mm. As presented in Table 6.4, a typical beam 35-50 ECT refers to a sandwich beam with 35 mm thick ECC strip on compression face and 50 mm thick ECC strip on tension face of masonry beam as core using epoxy as bonding agent. It is observed from Fig. 6.10 that for ECC strip with fixed thickness of 35 mm on compression face and epoxy being bonding agent, the load and deformation capacities of sandwich beam increase with increase in the thickness of precast ECC strip on the tension face. It may be noted that for ECC strip thickness of 40 mm and higher, the deformation capacity is almost same. However, increase in thickness of ECC strips on tension face cause delayed crushing of ECC strips on compression face. From Fig. 6.11, it is observed that with cement mortar as bonding agent, the load capacity of sandwich beam increases with increase in thickness of ECC strip on tension face, but with decreased deformation capacity. Thus it could be noted that epoxy as bonding material could be beneficial in terms of fabrication of sandwich masonry beams with ECC strips as facing structural elements for increased strength and deformability. However, when increased load capacity only is important, then cement mortar could also be used as bonding agent.

In case of masonry beams (Fig. 6.12) strengthened by precast ECC strips on tension face using epoxy as bonding agent, there is no change in the stiffness of tension strengthened beams with increasing thickness of ECC strip in tension. It may be attributed due to low tensile stiffness of epoxy bonded ECC. It is also noted that the maximum load and deformation capacities of tension strengthened beams are obtained for 45 mm thick ECC strip. Unlike tension strengthened beam with epoxy as bonding agent (Fig. 6.12), the use of cement mortar as bonding agent in tension strengthened beam (Fig. 6.13) in conjunction with increase in ECC strip thickness on tension face leads to the increase in the stiffness of tension strengthened beams. It may be noted that the cement mortar may play a role to increase the stiffness of tension strengthened beams using cement mortar

as bonding agent. This may be due to variation in thickness of cement mortar, leading to increase in stiffness of cement mortar bonded ECC.

In order to examine the effect of thickness of precast ECC strips on compression face of sandwich beams while keeping the tension face ECC strip thickness constant as 35 mm on the flexural response of the beams, thickness of precast ECC strip on compression face was changed from 20 to 50 mm using epoxy and cement mortar acting independently as bonding agent. It is observed from Fig. 6.14 that increase in the thickness of ECC strip on compression face beyond 20 mm with epoxy as bonding agent has no significant effect on flexural response of sandwich beams. Hence, 20 mm thickness of ECC strip could be considered as practical optimum thickness of ECC strip for bonding on compression face of sandwich masonry beams.

Unlike epoxy as bonding agent, use of cement mortar (see Fig. 6.15) helps in increasing the load capacity, stiffness, and deformation capacity of sandwich beam with increasing thickness of ECC strip on compression face. Although response of 40 and 45 mm thick ECC strips is same. Hence, it could be recommended that with cement mortar as bonding agent 40 mm thick precast ECC strip could be optimum for sandwich beam with 35 mm ECC strip on tension face.

Figures 6.16 and 6.17 show the effect of thickness of epoxy as bonding agent on the flexural responses of sandwich and tension strengthened beams, respectively. It is observed from Fig. 6.16 that the epoxy as bonding agent of thickness 0.5 mm results in the maximum peak load and deformation. Moreover, epoxy thickness in the range of 0.5 to 1 mm gives similar flexural response of sandwich beams. From Fig. 6.17, it is observed that there is no significant effect of epoxy bonding agent thickness on the flexural response of tension strengthened beams. However, as shown in Fig. 6.18, when cement mortar is used as bonding agent with thickness of range 2 to 10 mm, the maximum peak load of tension strengthened beam is observed for 2 mm thick cement mortar. Similar response is observed for sandwich beams also (see Fig. 6.19). However, the effect of cement mortar thickness is more appreciable in sandwich beam as observed for the epoxy as bonding agent. Thus, smaller the thickness (i.e., 2 mm) of cement mortar, the better will be the flexural response of tension strengthened as well as sandwich beams.

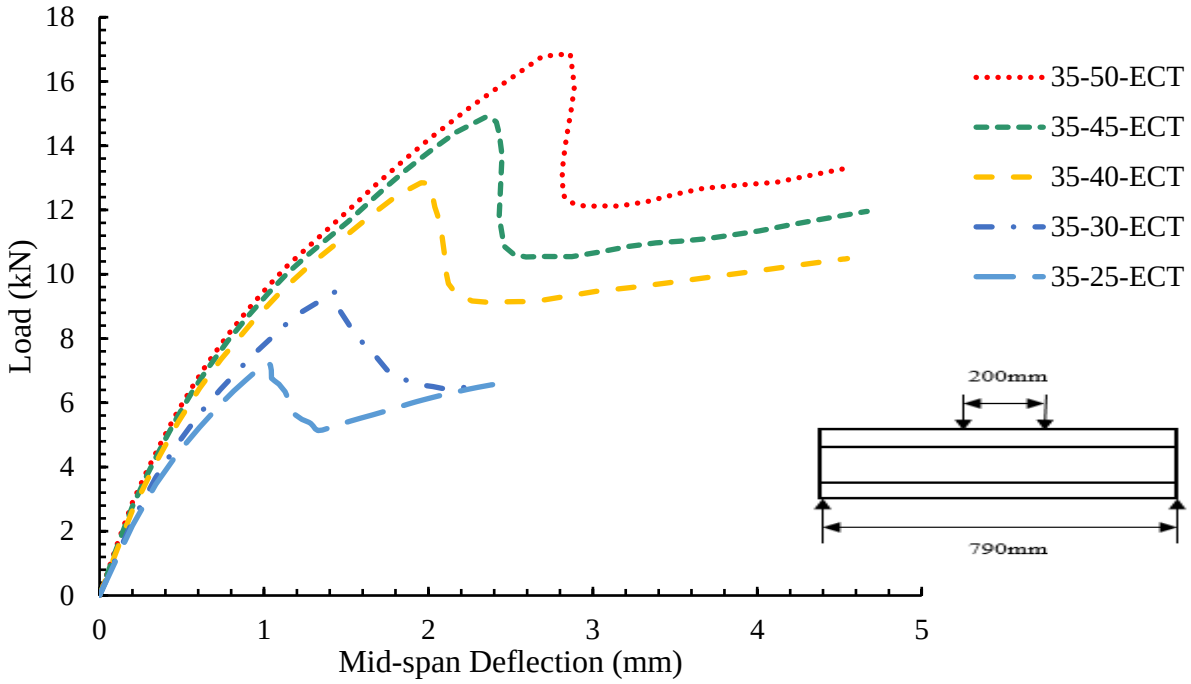

Fig. 6.10 Effect of thickness of tension face ECC on flexural response of sandwich beams with epoxy as bonding agent

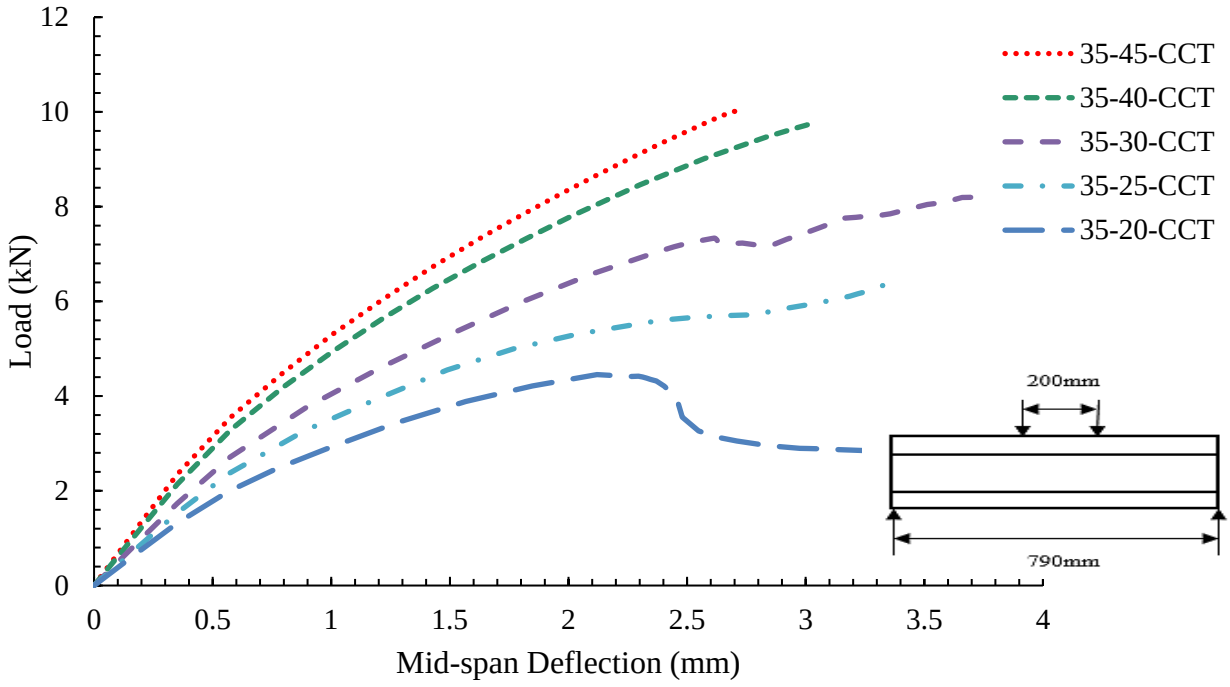

Fig. 6.11 Effect of thickness of tension face ECC on flexural response of sandwich beams with cement mortar as bonding agent

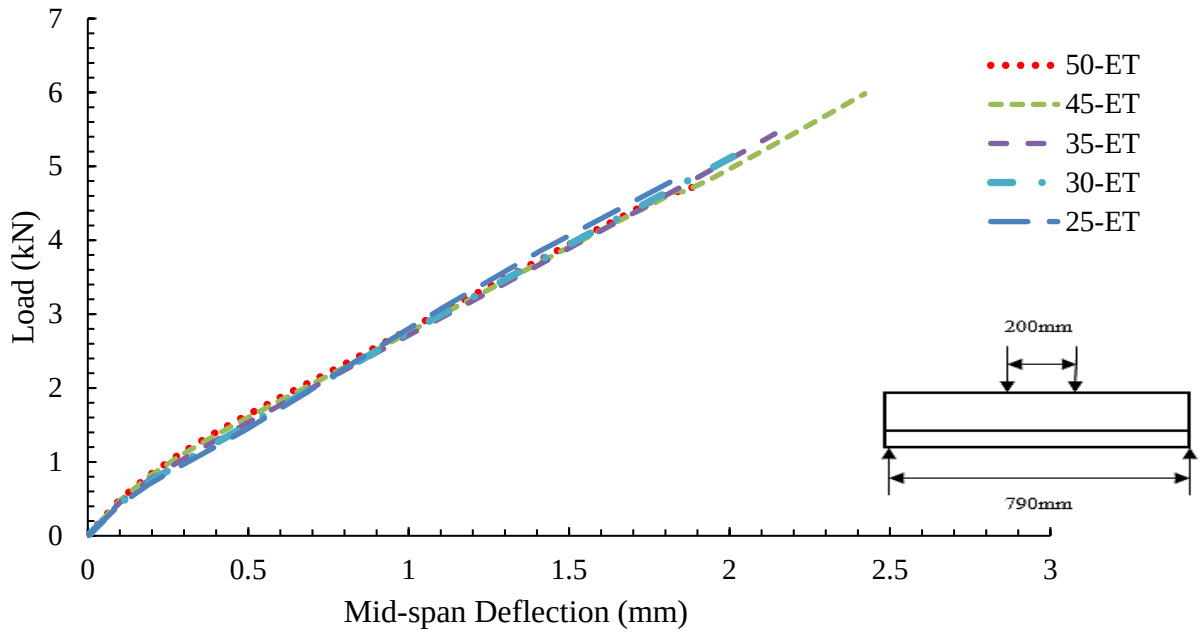

Fig. 6.12 Effect of thickness of tension face ECC on flexural response of tension strengthened beams with epoxy as bonding agent

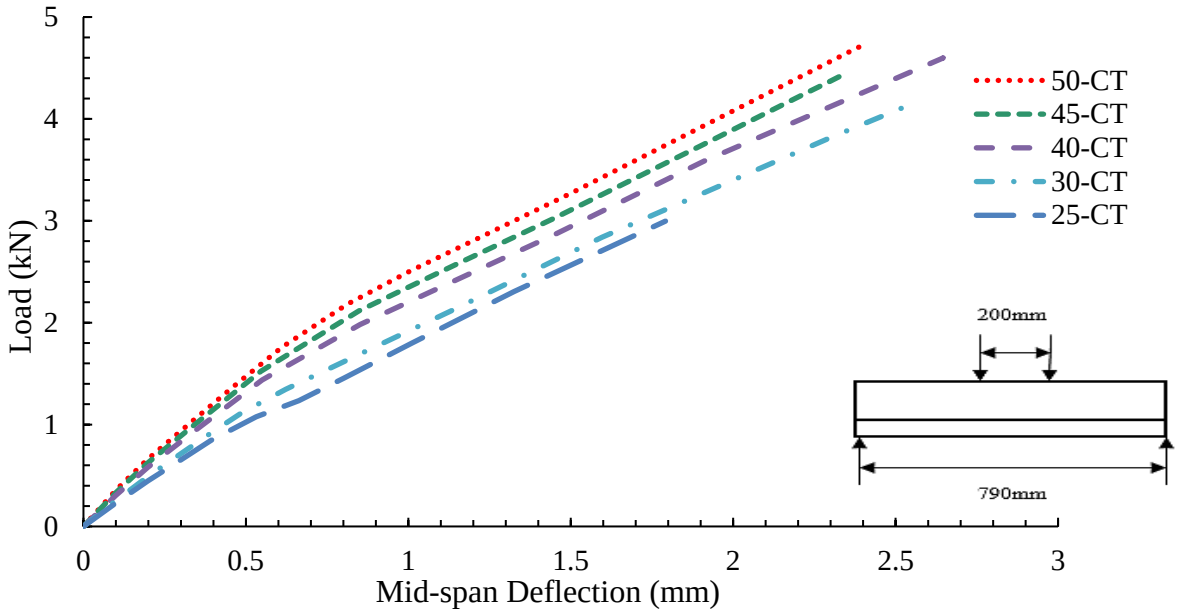

Fig. 6.13 Effect of thickness of tension face ECC on flexural response of tension strengthened beams with cement mortar as bonding agent

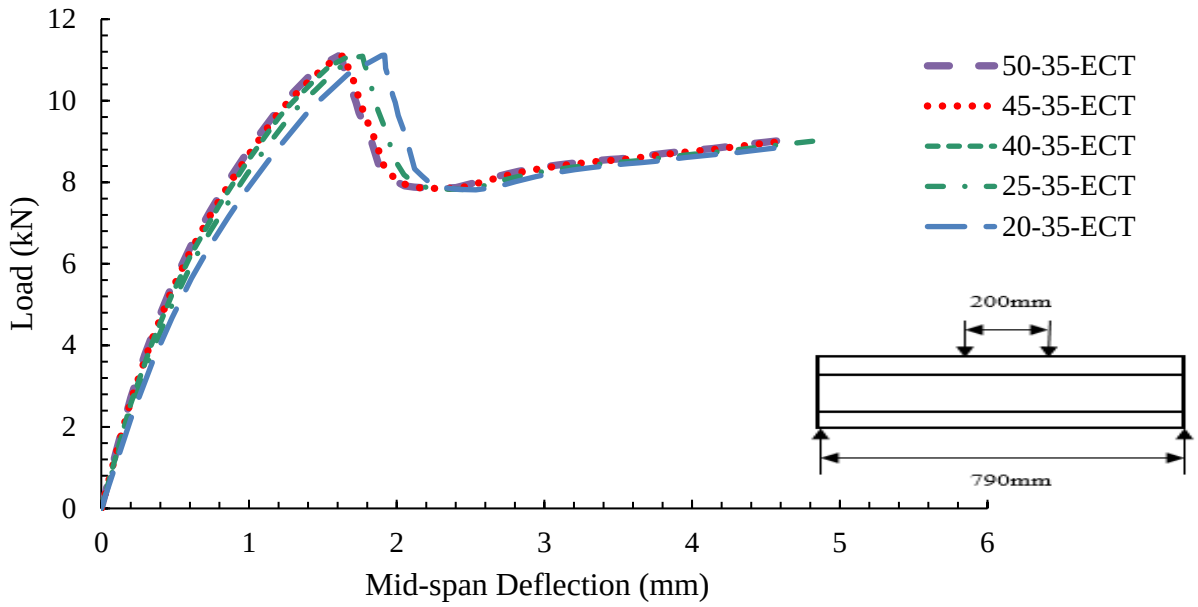

Fig. 6.14 Effect of thickness of compression faced ECC on flexural response of sandwich beams with epoxy as bonding agent

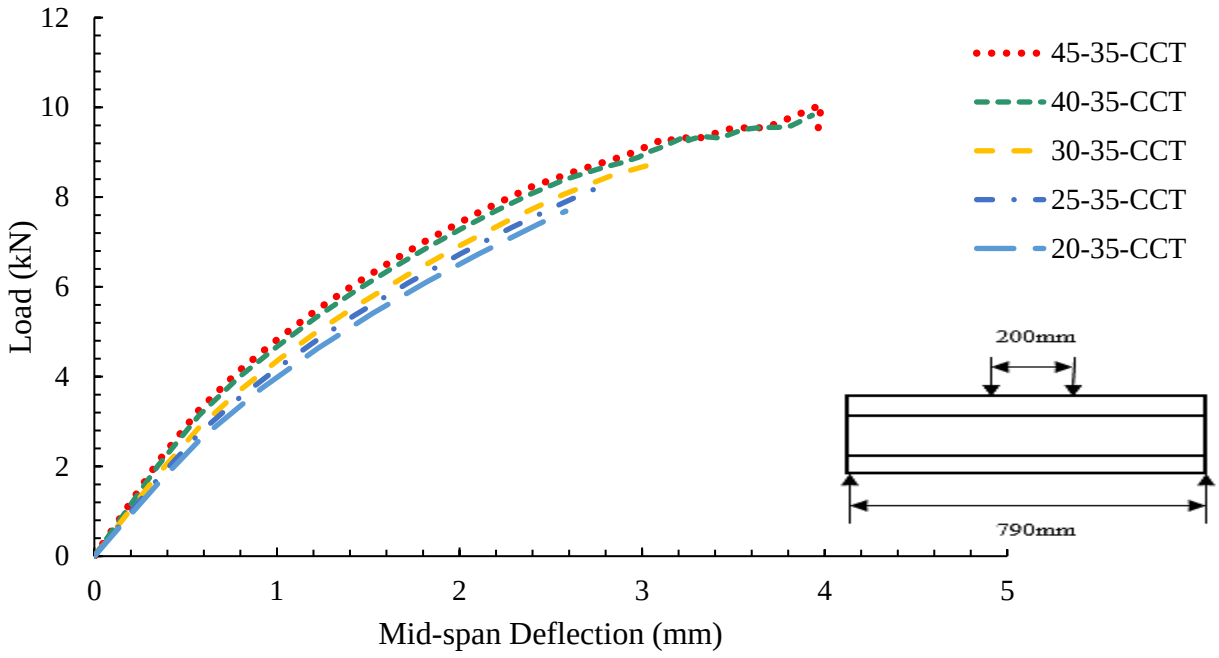

Fig. 6.15 Effect of thickness of compression faced ECC on flexural response of sandwich beams with cement mortar as bonding agent

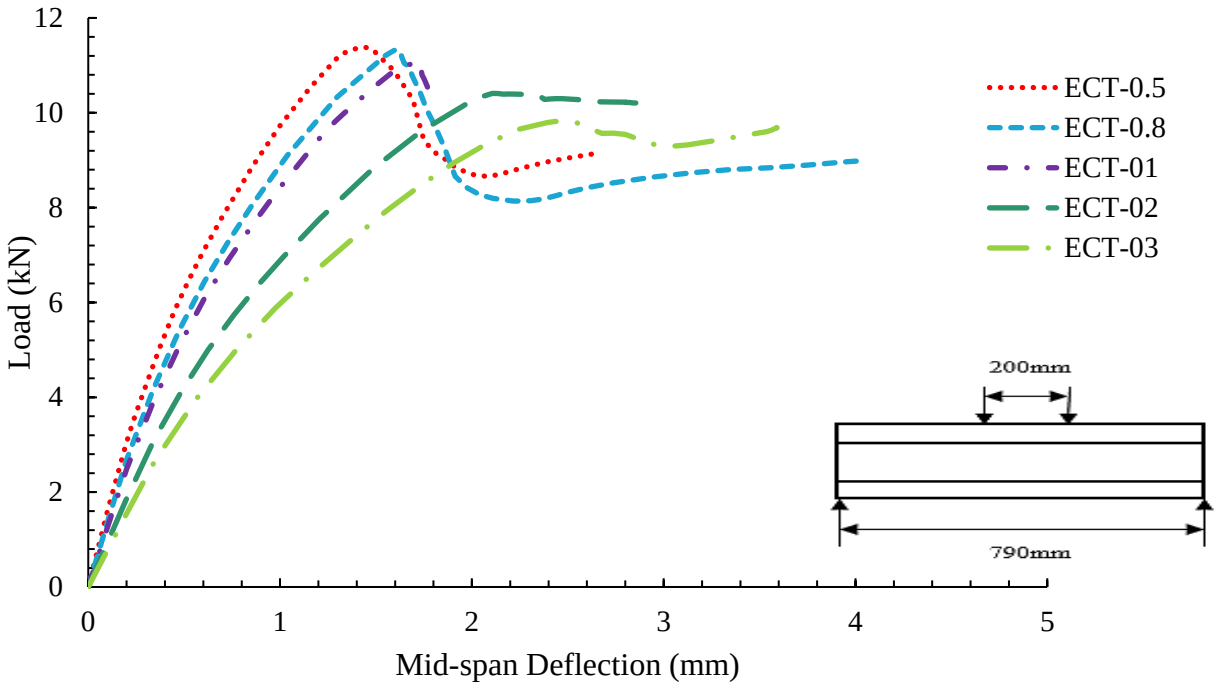

Fig. 6.16 Effect of bonding agent thickness on flexural response of sandwich beams with epoxy as bonding agent

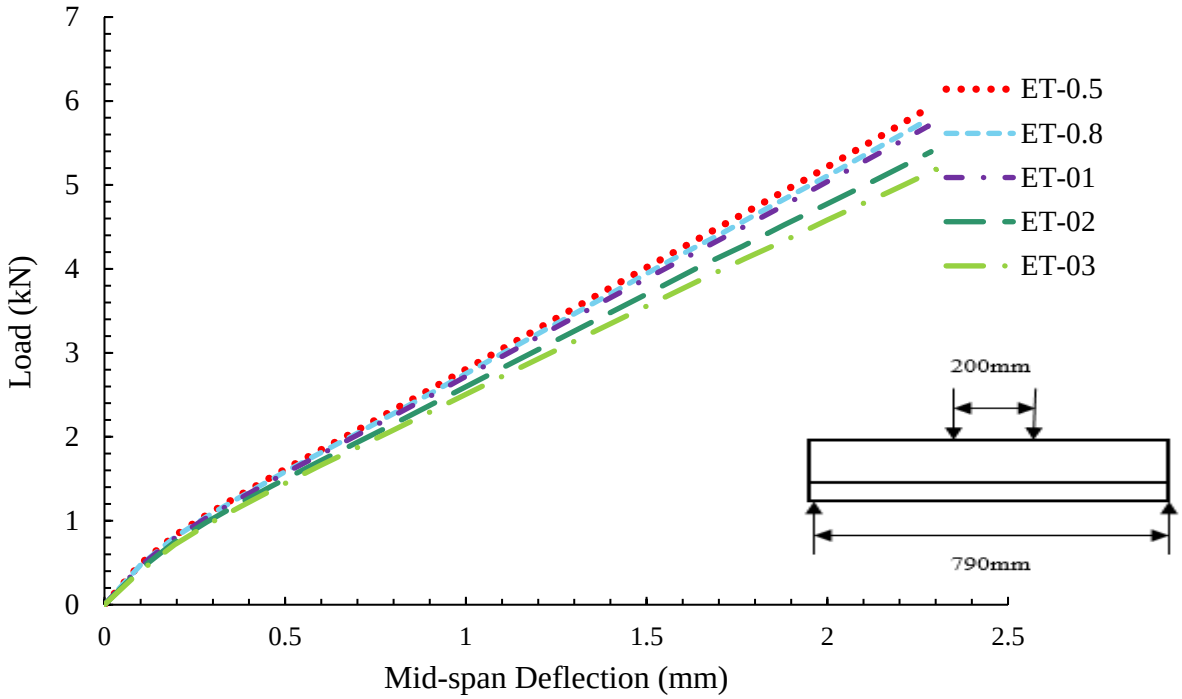

Fig. 6.17 Effect of bonding agent thickness on flexural response of tension strengthened beams with epoxy as bonding agent

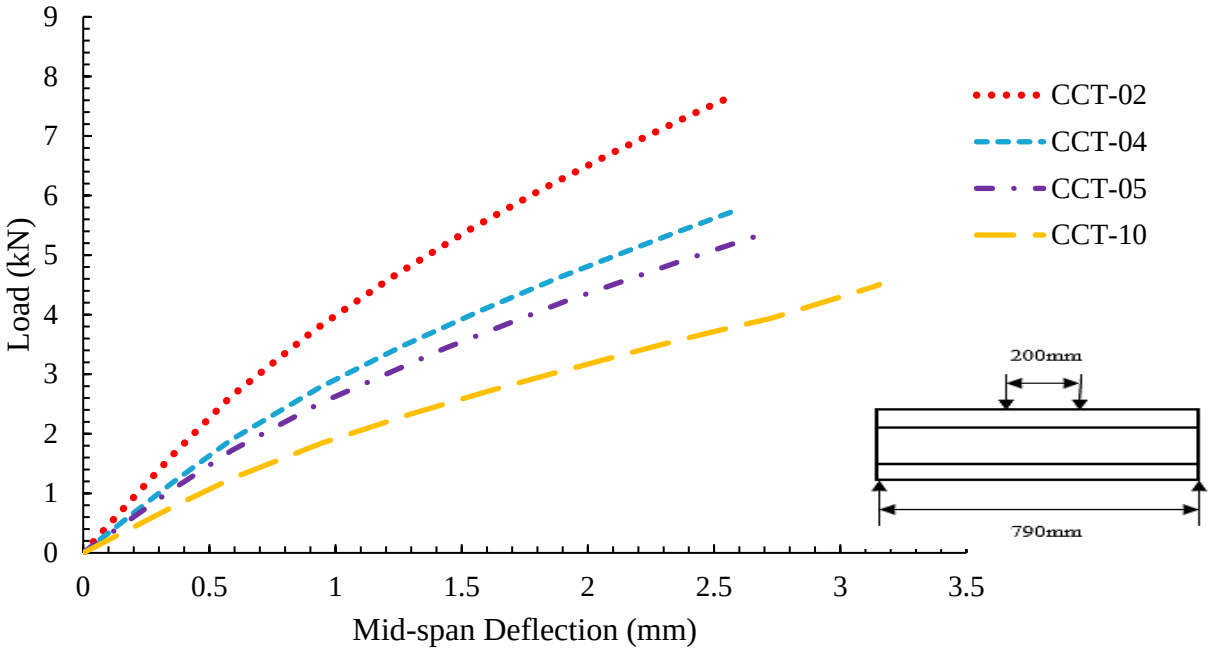

Fig. 6.18 Effect of bonding agent thickness on flexural response of tension strengthened beams with cement mortar as bonding agent

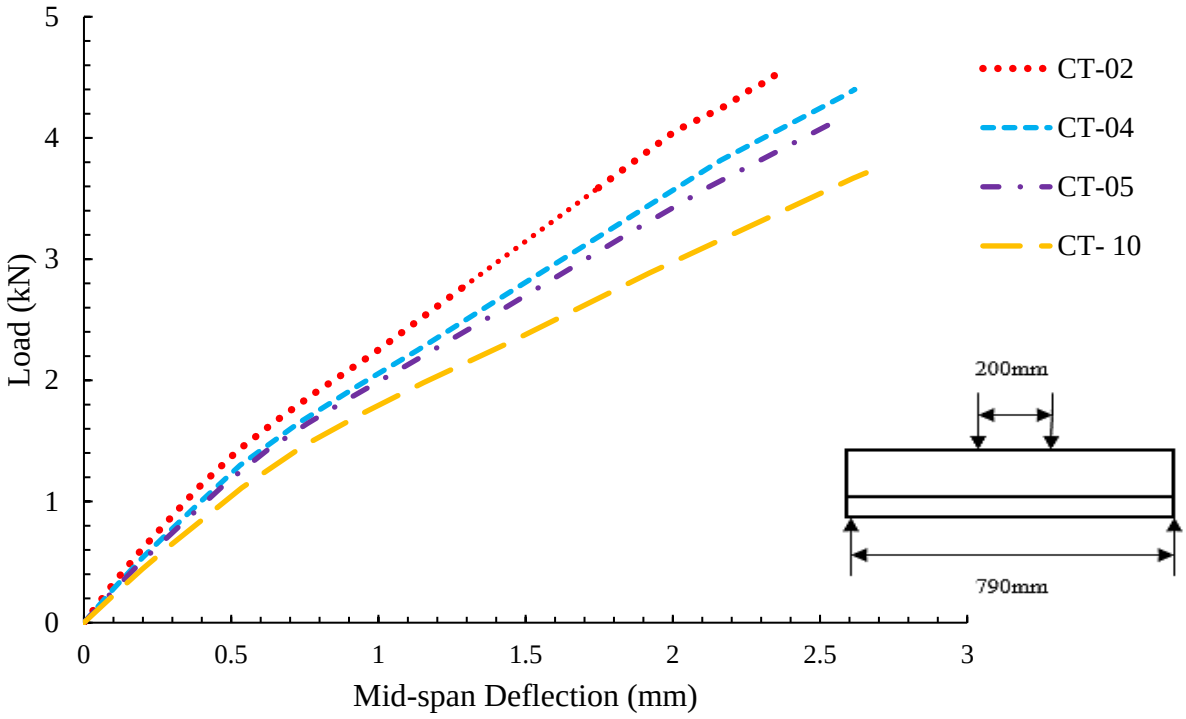

Fig. 6.19 Effect of bonding agent thickness on flexural response of sandwich beams with cement mortar as bonding agent

6.4 FE Models for ECC Strengthened Masonry Walls with and without Opening

This section demonstrates the numerical modelling of ECC strengthened masonry walls with and without opening. The experimental details of these masonry walls are explained in Chapter 5 (Section 5.2). This section deals with the mesh sensitivity analysis, validation of numerical models with the experimental results and parametric study of strengthened masonry walls. Table 6.6 depicts the descriptions and nomenclature of walls used in the study. To distinguish the tested specimens, and analytically modeled specimens, the designation 'X-E' and 'X-A' are used, where 'X' indicates the specimens described in Table 6.6; 'E' stands for experimentally tested specimen; 'A' refers to the numerically modeled specimen.

6.4.1 Mesh sensitivity

The mesh sensitivity analysis is very important aspect of the numerical modelling, especially for damage plasticity model, in the sense that the analysis does not converge to a unique solution as the mesh refinement leads to narrower crack bands. The influence of the mesh refinement with element size equal to 5, 10, 15, 20, and 50 mm on the behavior of the masonry walls and ECC sheets was examined. In addition, the computation time required for different mesh sizes is also considered. Consequently, the system used for sensitivity analysis had the configuration of Intel(R) Core(TM) i7-4790 CPU @ 3.60GHz, 4 Core(s), 8 Logical Processor(s) with 32 GB of RAM memory working with Windows7 64 bits. Figures 6.20 and 6.21 show respectively the normalized load (ratio of numerical load (P_{num})/experimental load (P_{exp})) versus mid-span deflection curves for masonry and ECC. In the graph legend, 'M-5' stands for element size of 5 mm and value in parentheses represents the computational time taken for that element size. The predicted normalized load increases slightly as the mesh size reduces up to certain limit. Considering the normalized load (numerical value/experimental value), the element sizes of 20 mm and 10 mm have shown the better compromise (value nearest to 1) in the case of masonry walls (Fig. 6.20) and ECC sheet (Fig. 6.21), respectively. All subsequent analyses of ECC strengthened masonry walls with and without opening were conducted using these mesh sizes, i.e., 20 mm for masonry and 10 mm for ECC sheet. It is observed that ECC sheet modeling requires smaller mesh size (10 mm) to achieve convergence due to its requirement of more nodal points than masonry. The epoxy was modeled as cohesive element in between the masonry wall and ECC sheet. The fine-meshed cohesive elements compared to solid elements has better convergence rate of solution as found

from the sensitivity analysis. The meshing size of 5 mm for cohesive elements (epoxy) was found most suitable for this study in terms of convergence. A typical meshed ECC strengthened masonry wall with and without opening is shown in Fig. 6.22 & 6.23, respectively.

Table 6.6 Details of masonry wall specimens

Sr. No.	Wall designation	Wall description*
1.	MW-A, MW-E	Control/unstrengthened masonry wall
2.	MWO-A, MWO-E	Control/unstrengthened masonry wall with opening at center
3.	ECC-A, ECC-E	Control ECC sheet of depth 25 mm
4.	ECCO-A, ECCO-E	Control ECC sheet of depth 25 mm with opening at center
5.	FW-A, FW-E	Flexural strengthened masonry wall with ECC sheet of thickness 25 mm
6.	FWO-A, FWO-E	Flexural strengthened masonry wall with ECC sheet of thickness 25 mm with opening at center
7.	FWT-10, FWT-25, FWT-50, FWT-75, FWT-100, FWT-150	Flexural strengthened masonry wall with ECC sheet of thickness 10, 25, 50, 75, 100, and 150 mm, respectively
8.	FWL-762, FWL-1000, FWL-1250, FWL-1500	Flexural strengthened masonry wall of length 762, 1000, 1250, and 1500 mm, respectively with ECC sheet of thickness 25 mm.
9.	FWW-480, FWW-750, FWW-1000	Flexural strengthened masonry wall of width 480, 750, and 1000 mm, respectively with ECC sheet of thickness 25 mm.

10.	FWOT-10, FWOT-25, FWOT-50, FWOT-75, FWOT-100, FWOT-150	Flexural strengthened masonry wall with ECC sheet of thickness 10, 25, 50, 75, 100, and 150 mm, respectively with opening at the center
11.	FWOL-762, FWOL-1000, FWOL-1250, FWOL-1500	Flexural strengthened masonry wall of length 762, 1000, 1250, and 1500 mm, respectively with opening at the center
12.	FWOW-480, FWOW-750, FWOW-1000	Flexural strengthened masonry wall of width 480, 750, and 1000 mm, respectively with opening at the center
13.	SOC (100 × 100), SOC (160 × 160), SOC (200 × 200), SOC (252 × 252)	Flexural strengthened masonry wall with square opening at the center of size 100 × 100, 160 × 160, 200 × 200, and 252 × 252 mm, respectively
14.	ROC (252 × 50), ROC (252 × 100), ROC (252 × 200), ROC (252 × 300)	Flexural strengthened masonry wall with rectangular opening at the center of size 252 × 50, 252 × 100, 252 × 200, and 252 × 300 mm, respectively
15.	LTO (160 × 160), LCO (160 × 160), MTO (160 × 160), MCO (160 × 160)	Flexural strengthened masonry wall with opening of size 160 × 160 at the left top corner, left center corner, middle top corner, and middle center corner of the wall, respectively

*In specimen designated as X-A or X-E, 'X' refers to specimens described; 'E' stands for experimentally tested specimen; 'A' refers to the numerically modelled specimen.

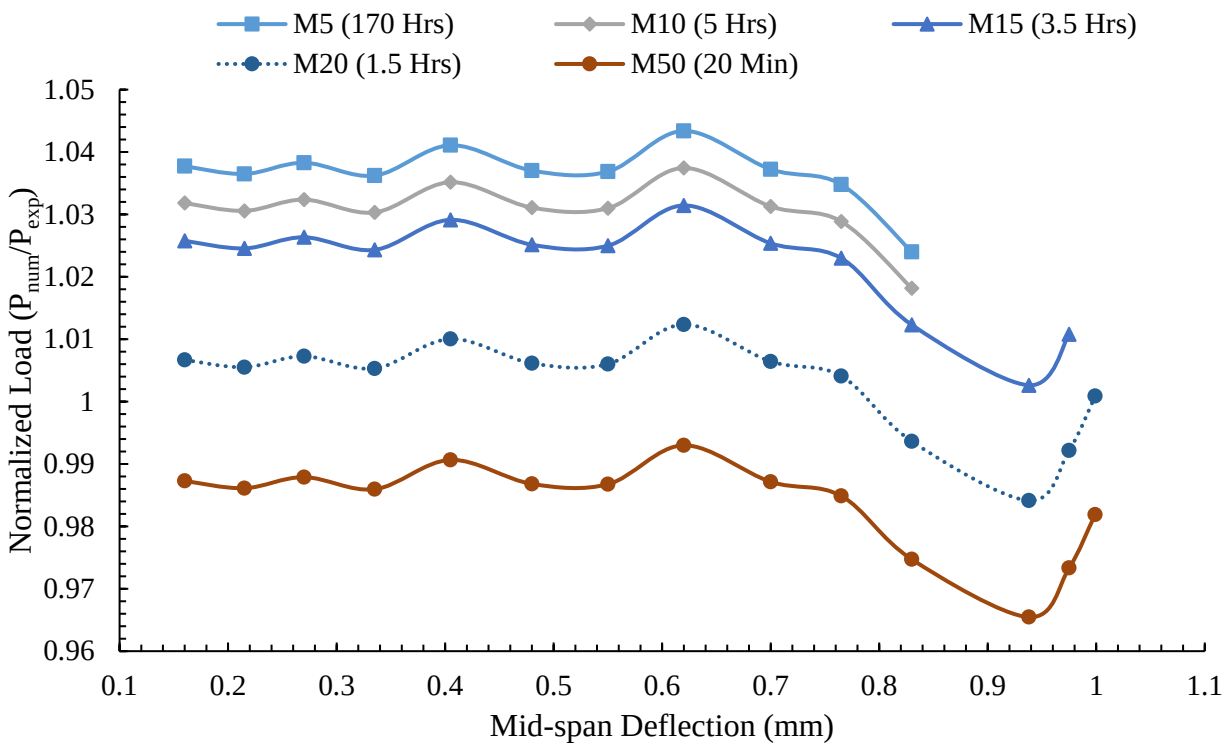

Fig. 6.20 Mesh sensitivity analysis of control masonry wall (MW-A)

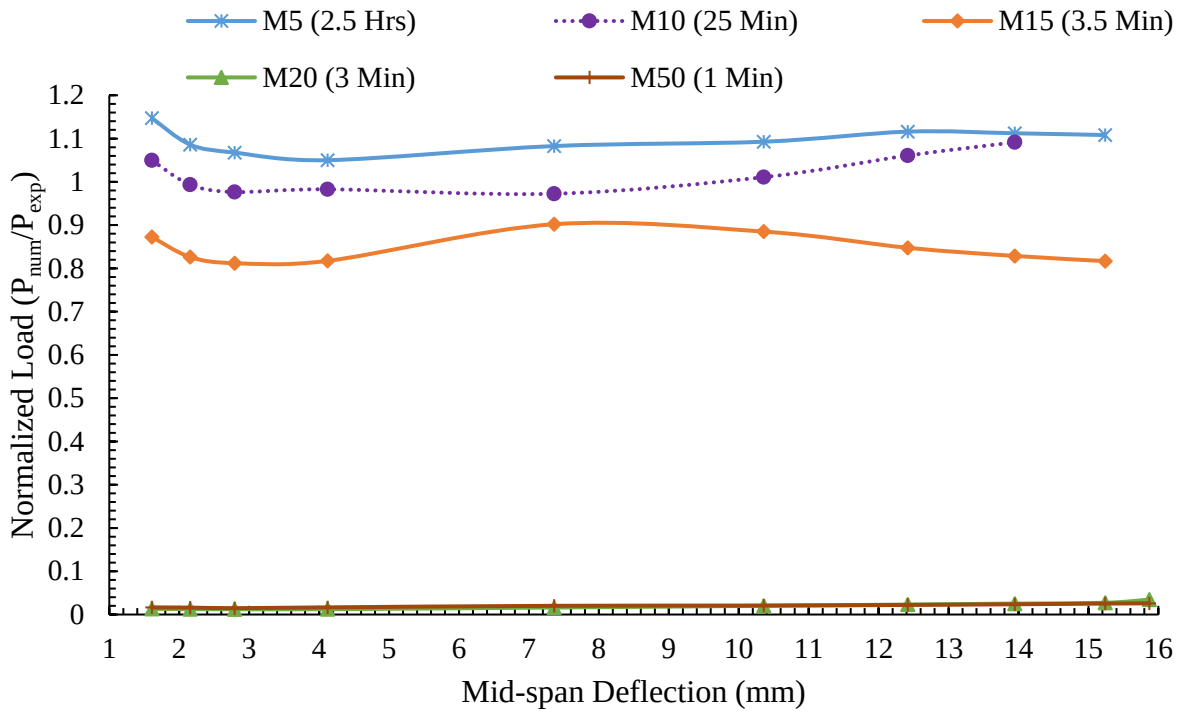

Fig. 6.21 Mesh sensitivity analysis of ECC sheet (ECC-A)

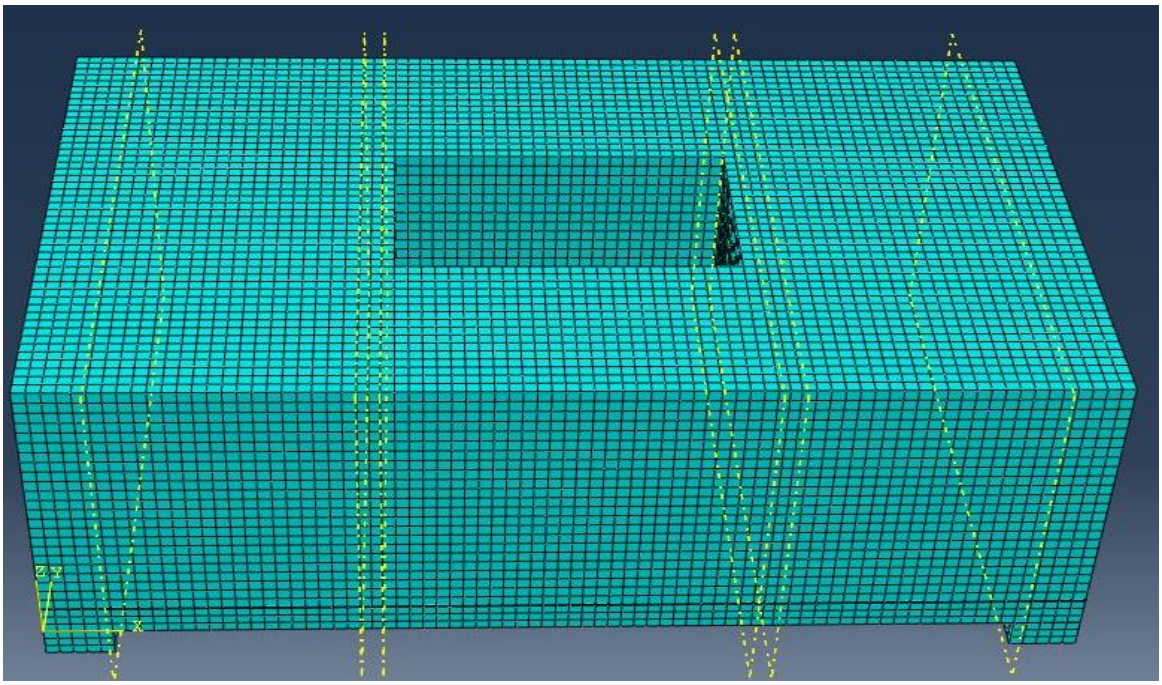

Fig. 6.22 Model of meshed ECC strengthened masonry wall with opening (FWO-A)

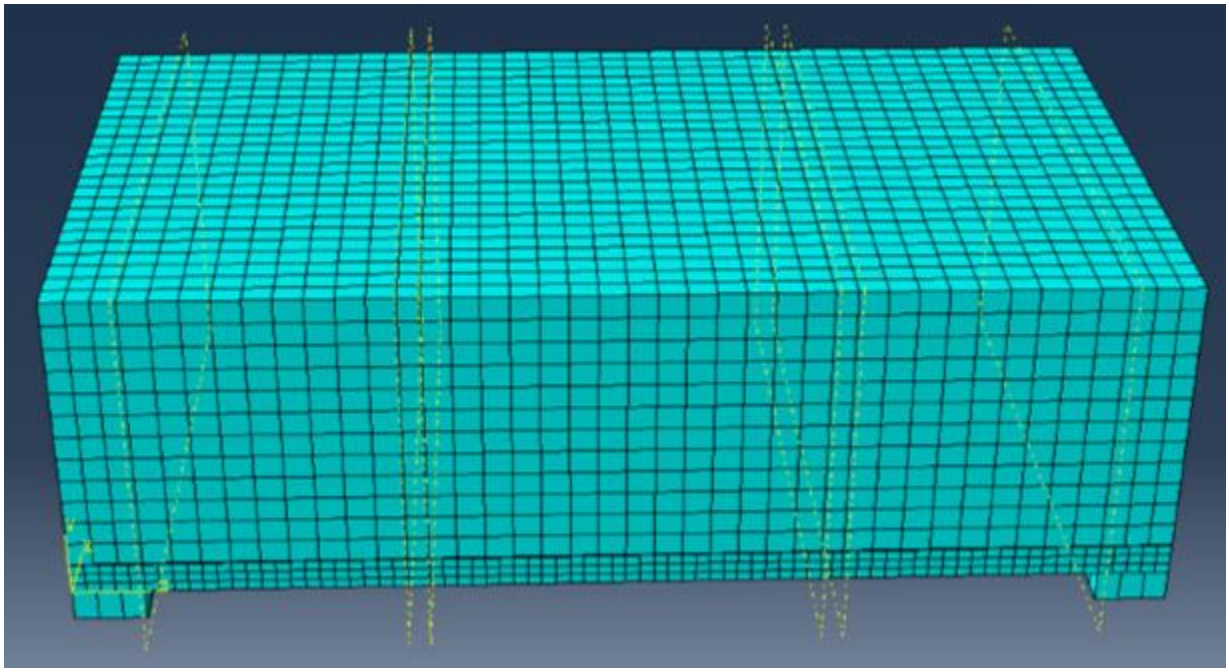

Fig. 6.23 Model of meshed ECC strengthened masonry wall (FW-A)

6.4.2 Validation of numerical modelling

In this section, details of comparison of results obtained using ABAQUS and experimental flexural response of unstrengthened/control and ECC strengthened masonry walls with and without opening are presented in Table 6.7. The average load-deflection response of experimentally tested and numerically modelled specimens of unstrengthened and strengthened masonry walls with and without opening is shown in Figs. 6.24-6.29. Figures 6.24 & 6.25 show the comparison of out-of-plane responses of unstrengthened masonry wall with and without opening, respectively obtained using ABAQUS (M20) and experimental four-point bending tests. It is observed that the flexural response of the unstrengthened masonry walls with and without opening is in close proximity to the corresponding experimental response with maximum deviation of 3.36% and 1.48% in the peak load, respectively. Similarly, it is shown in Figs. 6.26 and 6.27 that numerically (M10) and experimentally obtained out-of-plane response of ECC sheet of 25 mm thickness with and without opening are in close agreement. Thus, it is validated that the modelling of unstrengthened masonry walls and ECC sheets for out-of-plane loading using ABAQUS gives satisfactory results as they are close to the corresponding experimental results. The results obtained by ABAQUS for ECC strengthened masonry walls with and without opening are validated with the corresponding experimental results as shown in Figs. 6.28 and 6.29, respectively. It is seen that the numerical and experimental out-of-plane responses are in close proximity with maximum deviation of 7.47% and 4.32 % in peak load of ECC strengthened masonry wall with and without opening, respectively. However, the stiffness of numerically modelled walls is slightly more and may be attributed to pre-cracking flexural response not considered in the modelling. The nature of load versus deflection curve is observed to be similar. Figures 6.30 and 6.31, illustrates the deformed shape of ECC strengthened masonry wall with and without opening, respectively subjected to four-point loading.

Table 6.7 Validation of experimental results with numerical study

Wall designation*	Experimental		Numerical		% age error in peak load	% age error in mid-span deflection
	Peak load (kN)	Mid-span deflection (mm)	Peak load (kN)	Mid-span deflection (mm)		
MW	15.48	1.02	15.71	1.01	1.48	0.21
MWO	10.65	0.84	11.02	0.87	3.36	3.57
ECC	2.62	15.87	2.85	15.25	8.80	3.91
ECCO	1.60	10.69	1.66	10.58	3.66	1.03
FW	83.80	9.45	87.42	8.80	4.32	6.88
FWO	63.85	7.35	69.00	7.87	7.47	7.01

* Full description of wall designation is given in Table 6.6.

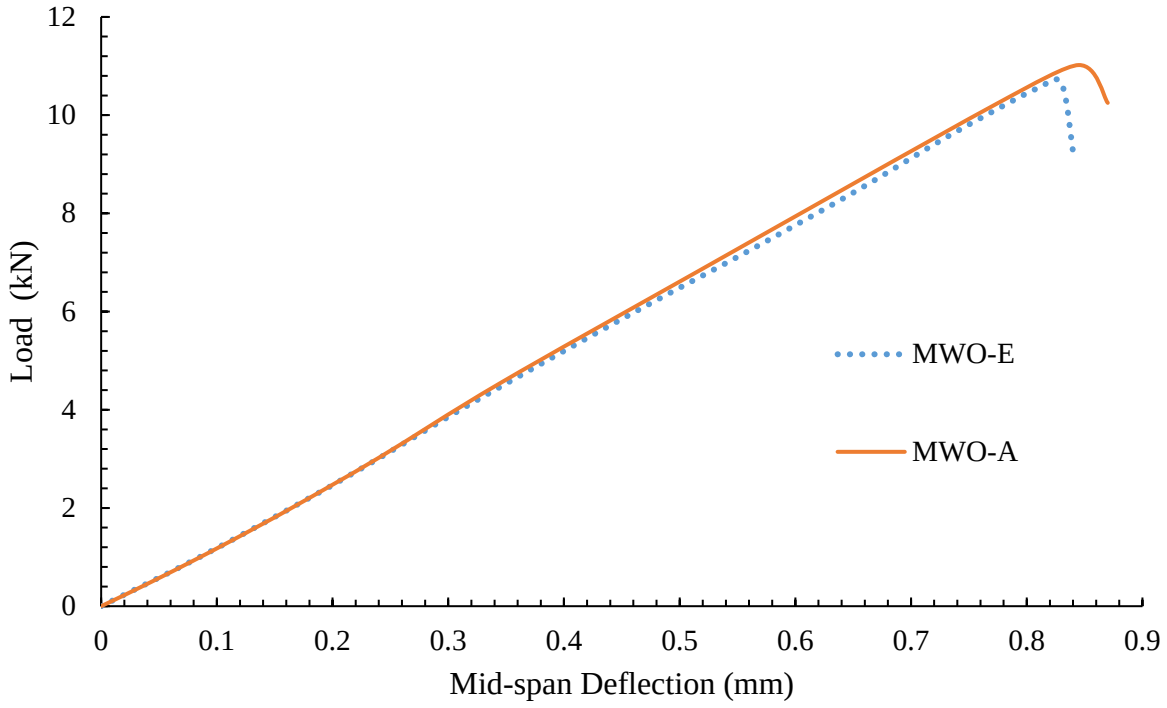

Fig. 6.24 Load-deflection response of control masonry wall with opening (MWO)

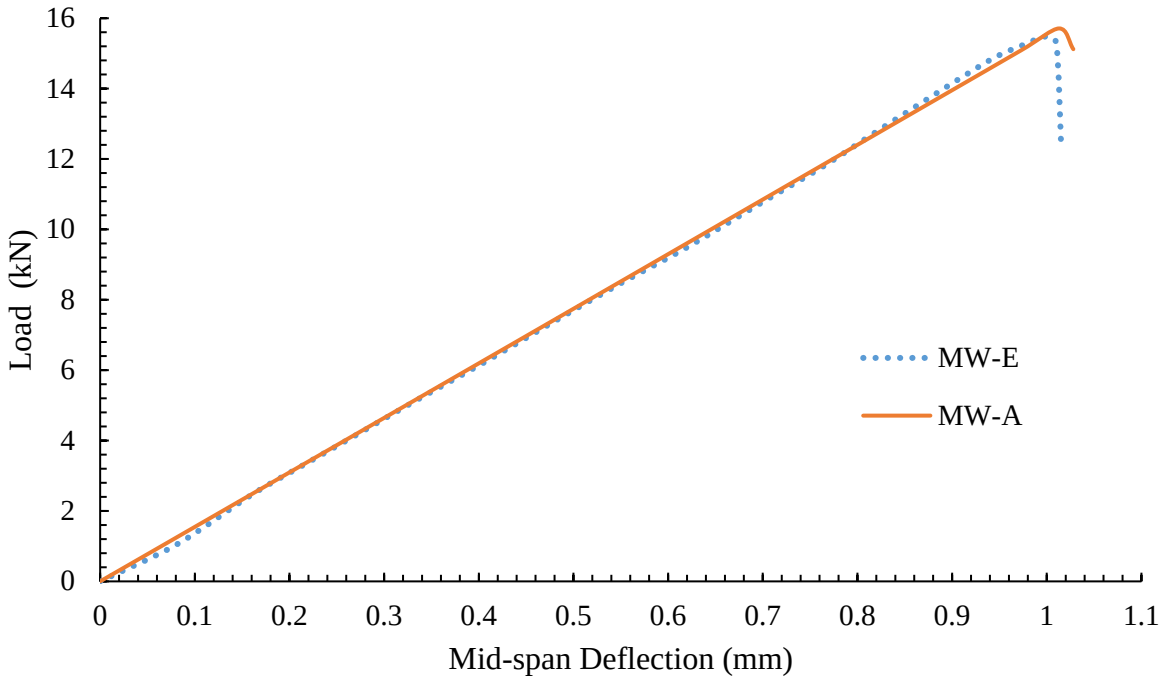

Fig. 6.25 Load-deflection response of control masonry wall without opening (MW)

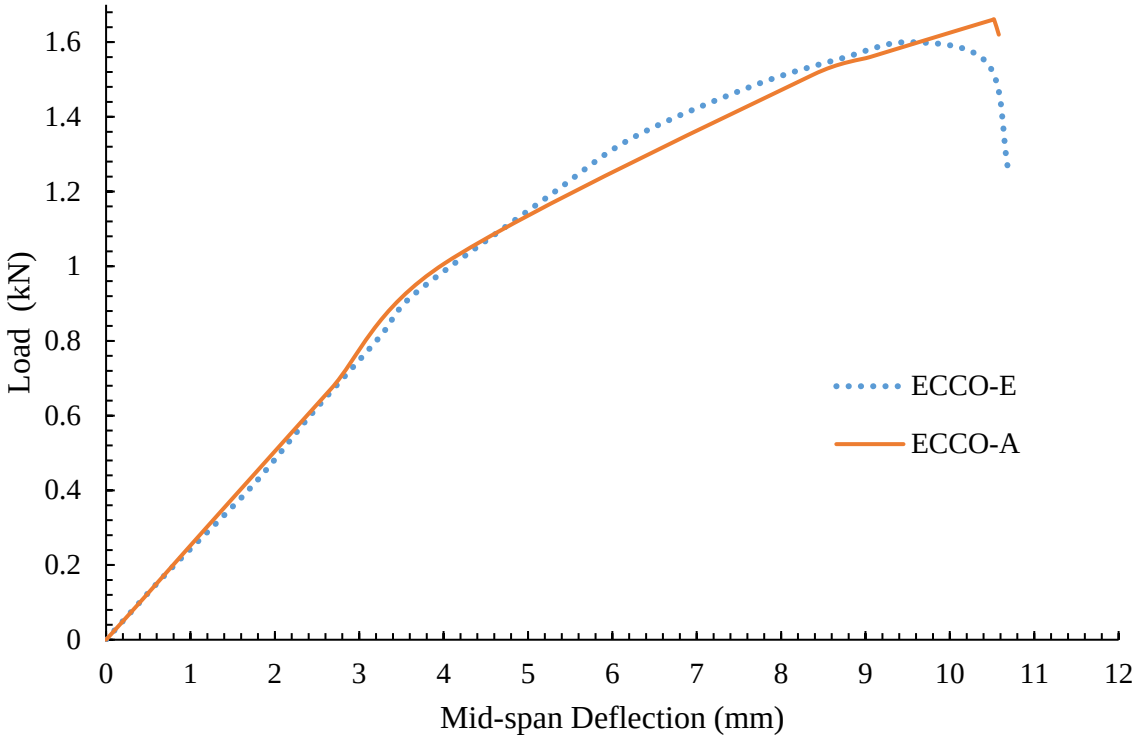

Fig. 6.26 Load-deflection response of ECC sheet with opening (ECCO)

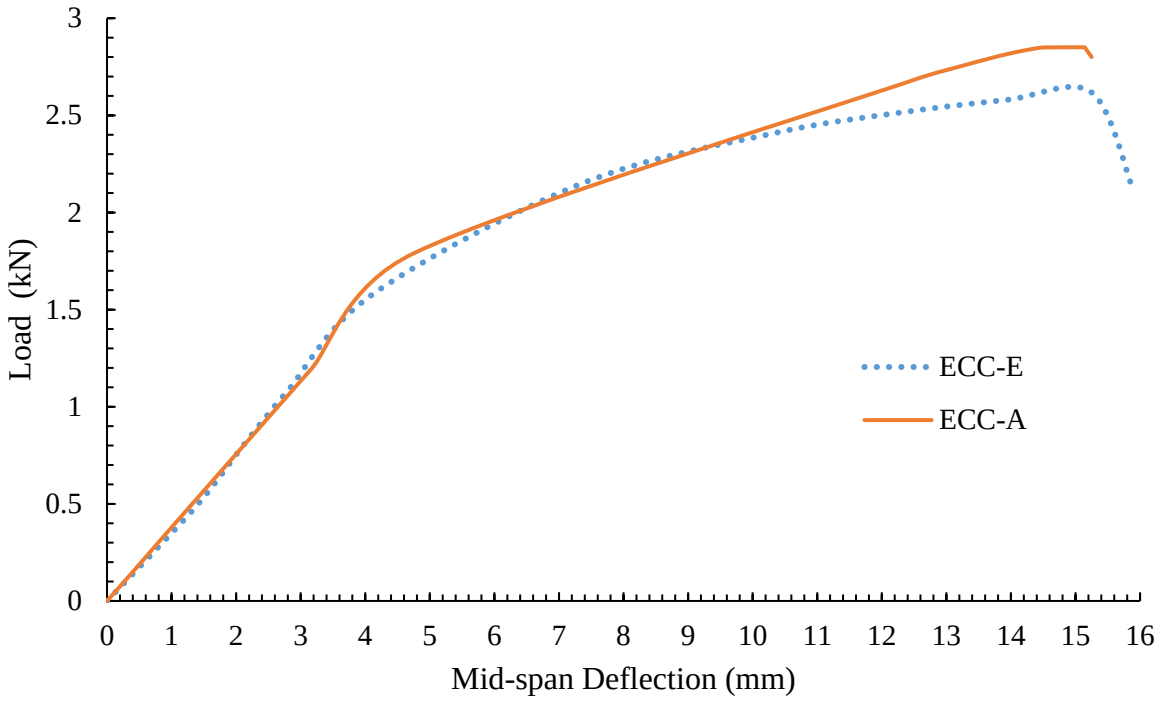

Fig. 6.27 Load-deflection response of ECC sheet without opening (ECC)

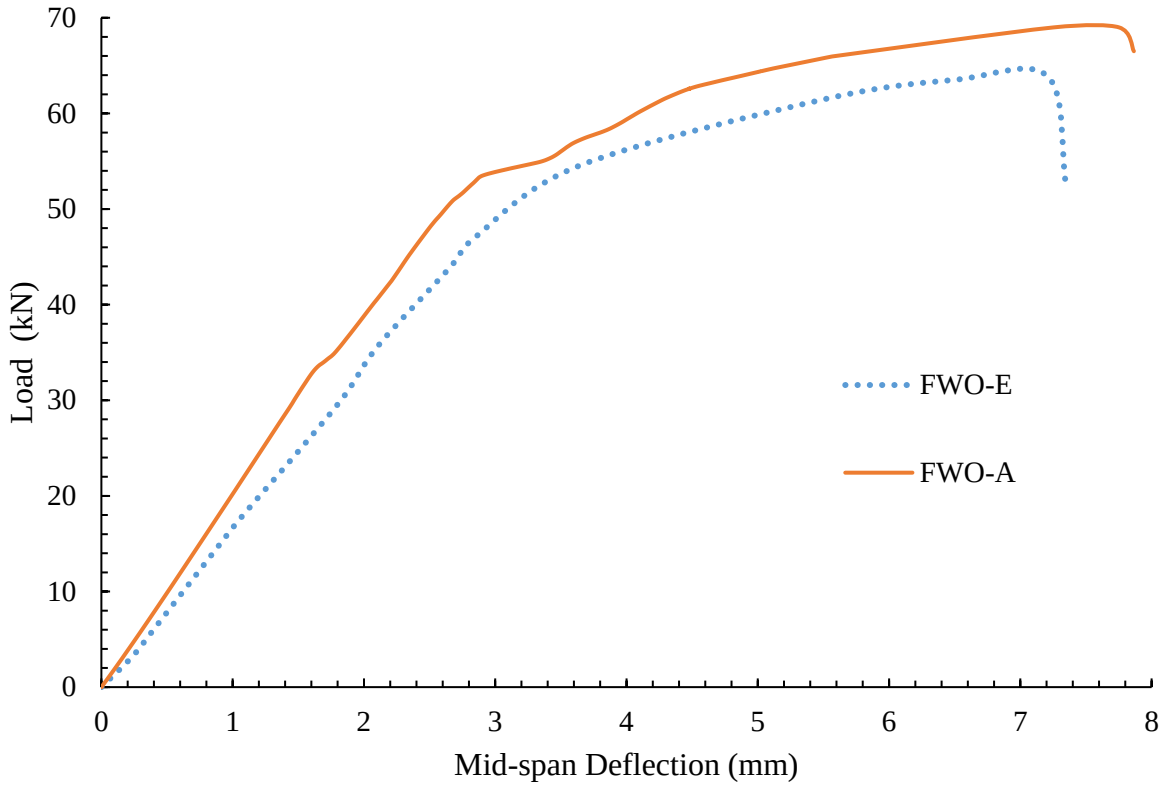

Fig. 6.28 Load-deflection response of ECC strengthened masonry wall with opening (FWO)

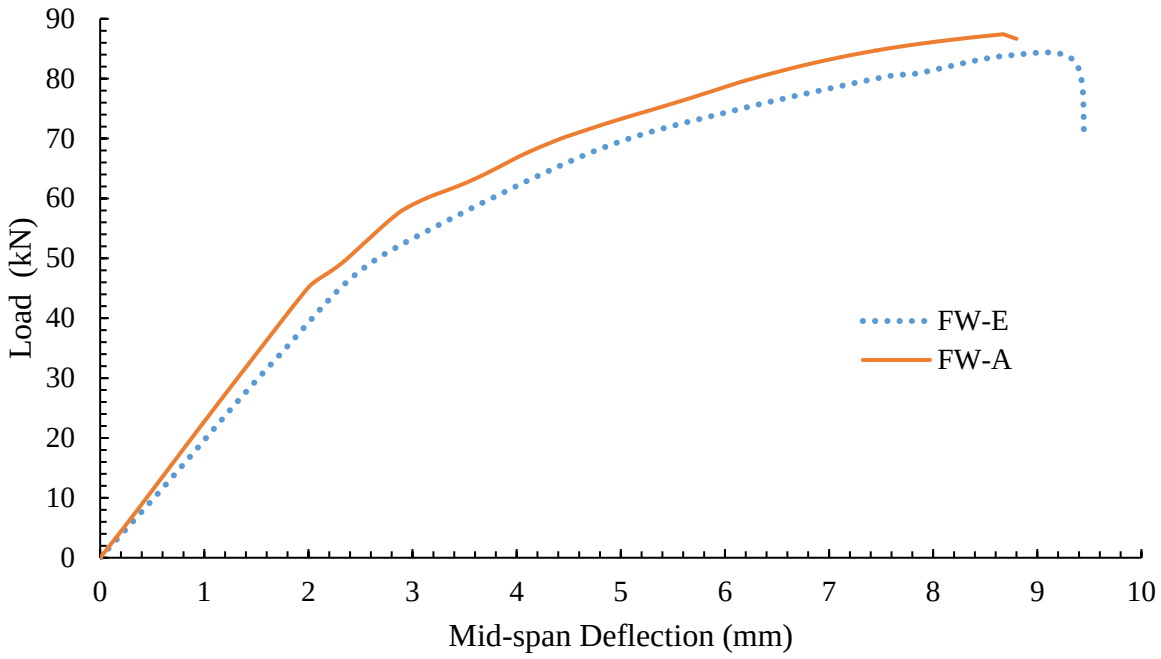

Fig. 6.29 Load-deflection response of ECC strengthened masonry wall (FW)

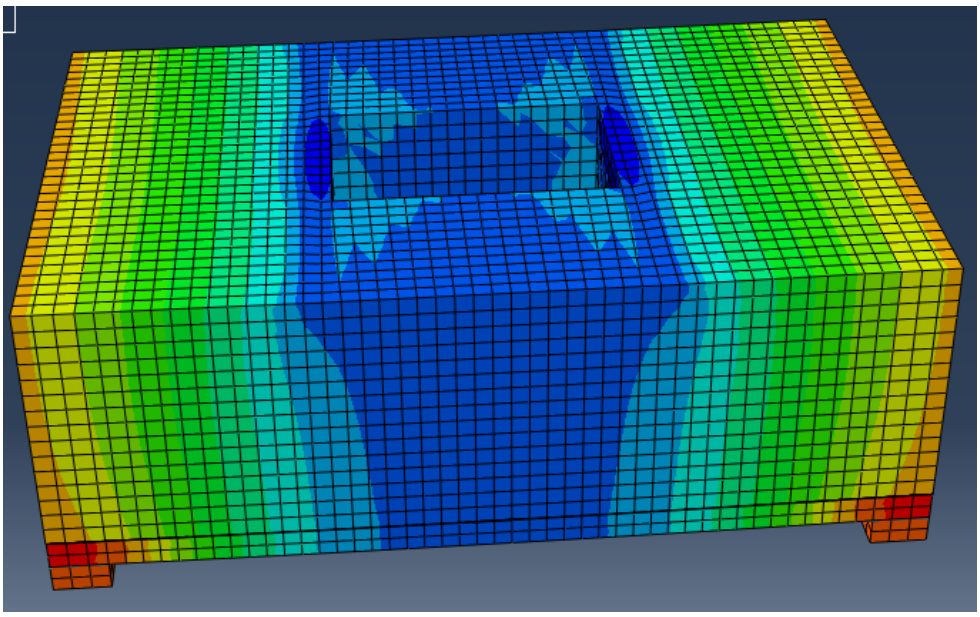

Fig. 6.30 Deformed shape of ECC strengthened masonry wall with opening (FWO-A)

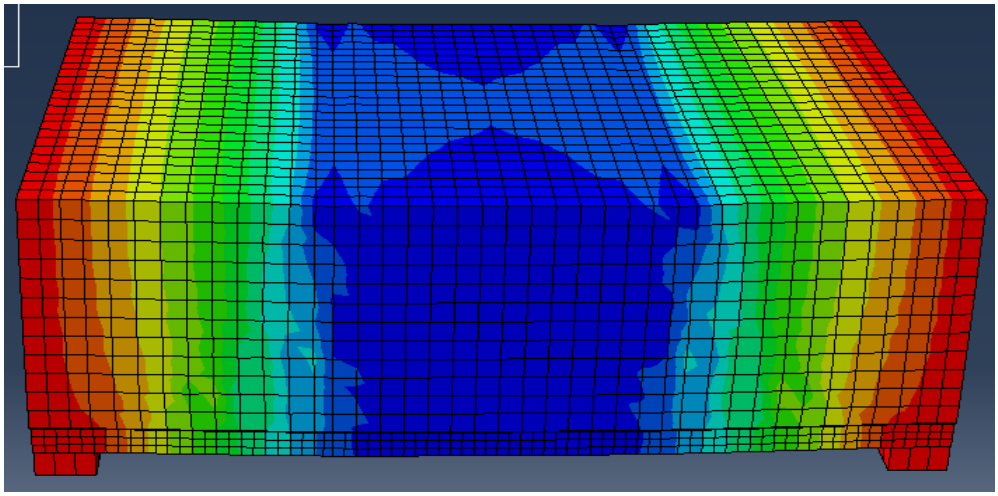

Fig. 6.31 Deformed shape of ECC strengthened masonry wall (FW-A)

6.4.3 Parametric study on ECC strengthened masonry wall without opening

The parametric study has been conducted by changing the various parameters such as thickness of ECC sheet, length, and width of the strengthened masonry walls to observe the effect of ECC reinforcement ratio, span to depth ratio (i.e. L/d), and width to thickness ratio (i.e., b/h) of strengthened wall. Serial numbers 7-9 in Table 6.6 provide a detailed nomenclature of the ECC strengthened masonry walls without opening analyzed in ABAQUS as a part of parametric study.

6.4.3.1 Results and discussions of ECC strengthened masonry wall without opening

In this section, results of parametric study of Serial numbers 7-9 in Table 6.6 obtained using ABAQUS are presented in Table 6.8 in terms of normalized flexural strength (M/f_mbd^2) and w_{max}/h. Here, M is the maximum bending moment at the mid-span of the wall; f_m is the masonry compressive strength; b is the width of specimen; d is the distance between the extreme compression fiber of masonry to the centroid of ECC sheet; w_{max} is the maximum mid-span deflection of the specimen; and h is the total depth of the strengthened specimens.

The effect of ECC reinforcement ratio for a fixed value of span and depth of masonry on the out-of-plane response of strengthened masonry walls is shown in Fig. 6.32. In the graph legend, 'FWT-10 (4.15%)', the FWT-10 stands for flexural strengthened masonry wall with 10 mm thick ECC sheet; value in parentheses represents ECC reinforcement ratio which is calculated by cross-sectional area of ECC over total cross-sectional area of strengthened masonry wall. It may be noted that graph is plotted between normalized flexural strength (M/f_mbd^2) and w_{max}/h to propose the

design chart of ECC strengthened masonry walls. It is observed that the value of $M/f_m bd^2$ of strengthened masonry walls (Fig. 6.32) increases with increase in the ECC reinforcement ratio, but with decreased value of w_{max}/h. Thus it could be noted that small percentage of ECC reinforcement ratio could be beneficial in terms of ductility. In order to examine the effect of L/d ratio while keeping the width and thickness of the specimens and ECC reinforcement ratio constant, the length of the specimens was changed from 762 mm to 1500 mm. It is observed from Fig. 6.33 that increase in the L/d ratio (i.e., 2.72 to 5.75) while keeping the constant ECC reinforcement ratio (9.77%) has significantly decreased the normalized flexural strength ($M/f_m bd^2$) for L/d=5.7. The w_{max}/h value has increased with increases of L/d ratio for a fixed value of flexural load. It is worth noting that for the lowest value of L/d ratio i.e., (L/d=2.72), the flexural stiffness is higher for the w_{max}/h value up to 0.01 and then drops to that for L/d = 5.75. This shows that for L/d=2.72, shear deformation becomes predominant and reduces the flexural strength.

Table 6.8 Results of parametric study of Serial numbers 7-9*

Sr. No.*	Wall designation	Normalized flexural strength $\left(\frac{M}{f_m bd^2}\right)$	$\frac{W_{max}}{h}$
7.	FWT-10	0.064	0.051
	FWT-25	0.080	0.034
	FWT-50	0.079	0.017
	FWT-75	0.084	0.015
	FWT-100	0.082	0.010
	FWT-150	0.093	0.009
8.	FWL-762	0.080	0.034
	FWL-1000	0.096	0.038
	FWL-1250	0.085	0.040
	FWL-1500	0.078	0.041
9.	FWW-480	0.080	0.034
	FWW-750	0.129	0.024
	FWW-1000	0.151	0.038

* Serial numbers as per Table 6.6.

Figure 6.34 shows the effect of width to thickness ratio (b/h) on the flexural response the wall. It is observed that for the lowest value of b/h (i.e., b/h=1.88), the normalized flexural strength ($M/f_m bd^2$) is the lowest for a particular deflection (i.e., w_{max}/h), while it is highest for b/h=2.93 but with reduced deflection. However, it may be noted that for b/h=3.91, there is remarkable increase in load capacity as well as deformation capacity. Thus it could be recommended that for b/h=3.91 beneficial for flexural strength of the wall.

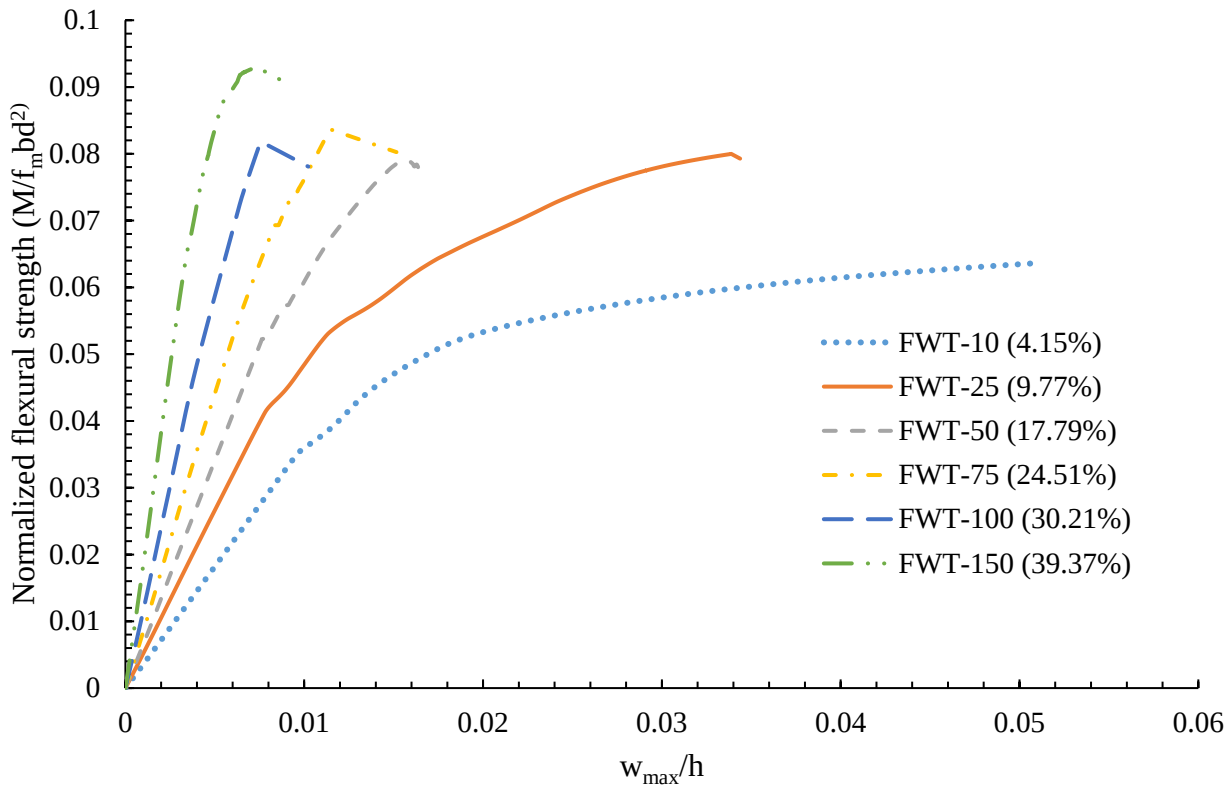

Fig. 6.32 Effect of ECC reinforcement ratio on flexural response of strengthened wall

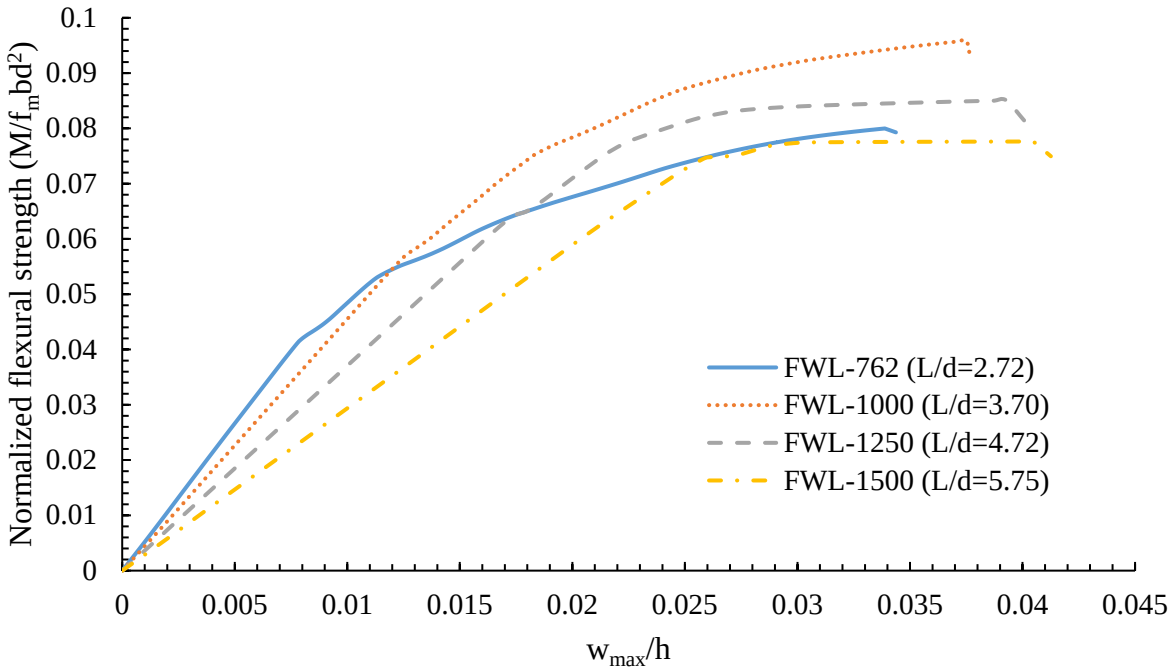

Fig. 6.33 Effect of L/d ratio on flexural response of strengthened masonry wall for ECC reinforcement ratio of 9.77%

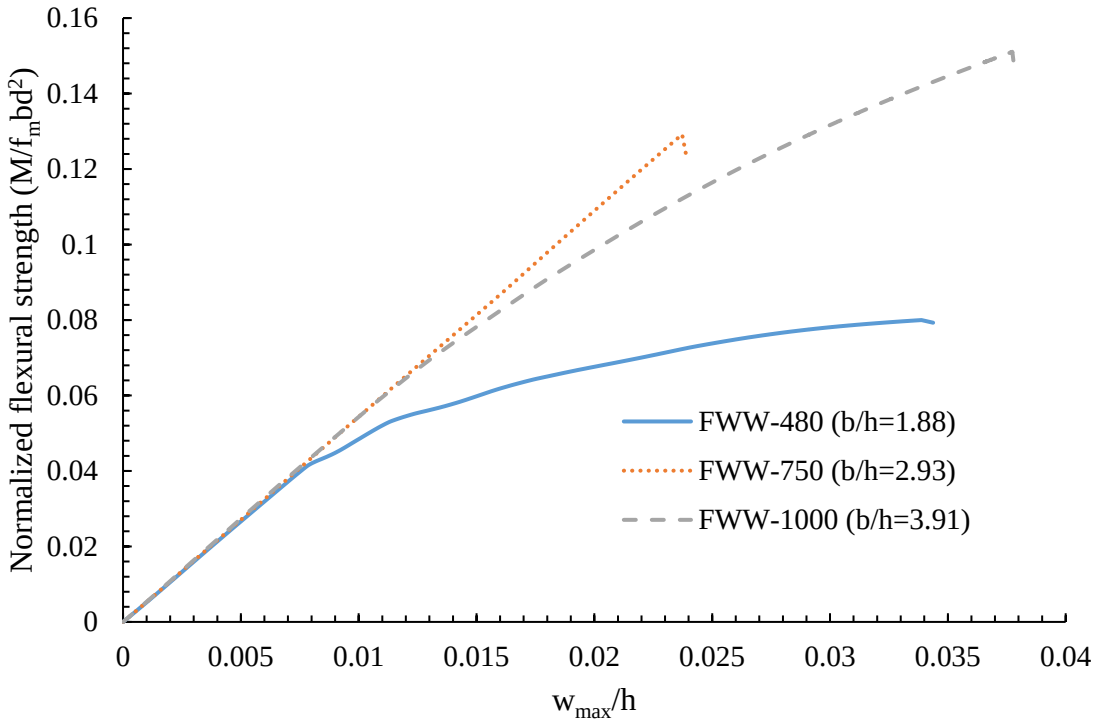

Fig. 6.34 Effect of b/h ratio on flexural response of strengthened masonry wall for ECC reinforcement ratio of 9.77%

6.4.4 Parametric study on ECC strengthened masonry wall with opening

Serial numbers 10-15 in Table 6.6 provide a detailed description of the ECC strengthened walls with opening analyzed in ABAQUS as a part of parametric study. The parametric study has been conducted by changing the various parameters such as thickness of ECC sheet, length, and width of the strengthened masonry walls with opening to observe the effect of ECC reinforcement ratio, span to depth ratio (i.e. L/d), and width to thickness ratio (i.e., b/h) of strengthened wall. It may be noted that the specimens corresponding to the Serial numbers 10-12 given in Table 6.6 have been provided with identical opening size of 252 × 160 mm. Furthermore, the research also considered varying opening dimensions in terms of square and rectangular opening. It also considers the position of openings at different location with constant dimension of 160 × 160 mm. Moreover, it may also be noted that the size of strengthened masonry walls (762 × 480 × 230 mm) has been kept constant while analyzing the effect of opening dimensions with varying opening ratio (Serial numbers 13 to15 in Table 6.6). The schematic diagrams with opening details (Serial numbers 13 to15) have been shown below in Figs. 6.35, 6.36, and 6.37, respectively.

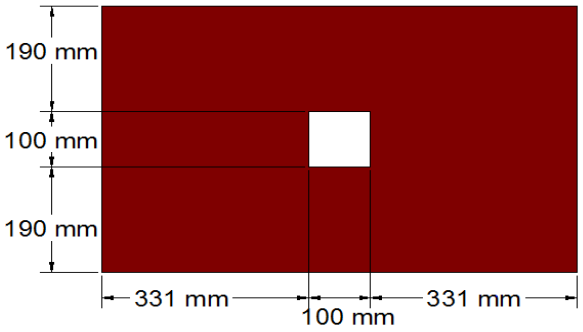

Fig. 6.35 (a) Masonry wall with opening at the center of size 100 × 100

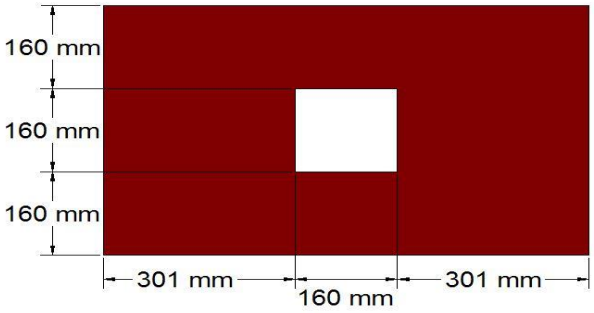

Fig. 6.35 (b) Masonry wall with opening at the center of size 160 × 160

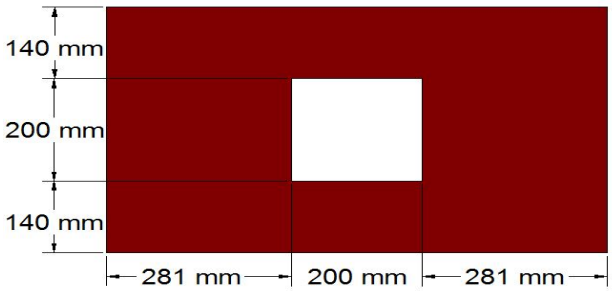

Fig. 6.35 (c) Masonry wall with opening at the center of size 200 × 200

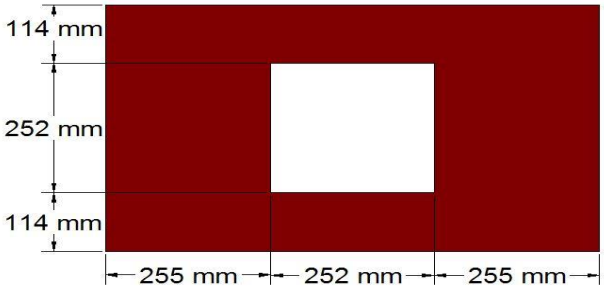

Fig. 6.35 (d) Masonry wall with opening at the center of size 252 × 252

Fig. 6.35 Flexural strengthened masonry wall with square opening at the center

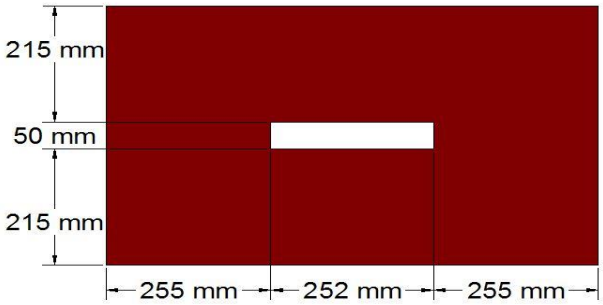

Fig. 6.36 (a) Masonry wall with opening at the center of size 252 × 50

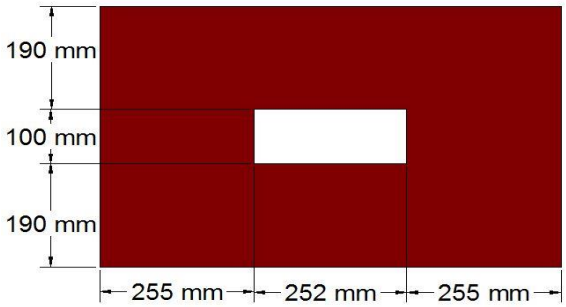

Fig. 6.36 (b) Masonry wall with opening at the center of size 252 × 100

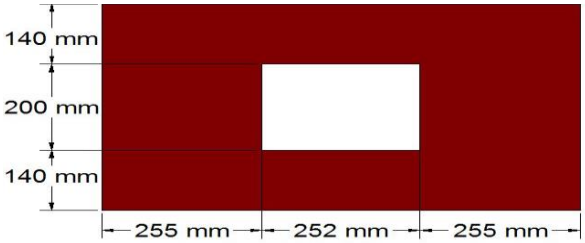

Fig. 6.36 (c) Masonry wall with opening at the center of size 252 × 200

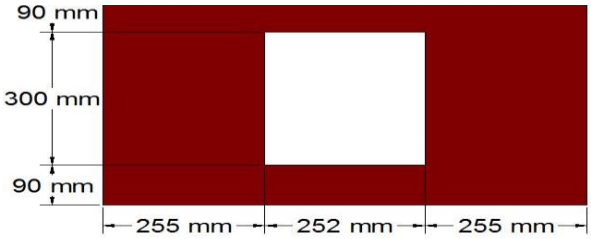

Fig. 6.36 (d) Masonry wall with opening at the center of size 252 × 252

Fig. 6.36 Flexural strengthened masonry wall rectangular with opening at the center

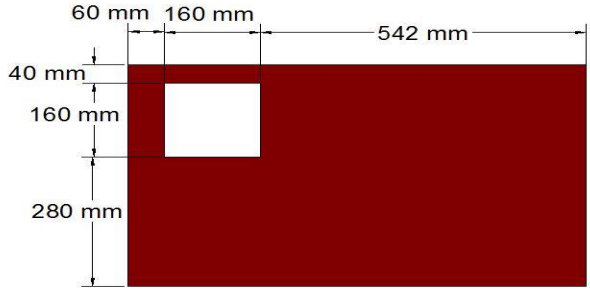

Fig. 6.37 (a) Left top opening in the wall (LTO)

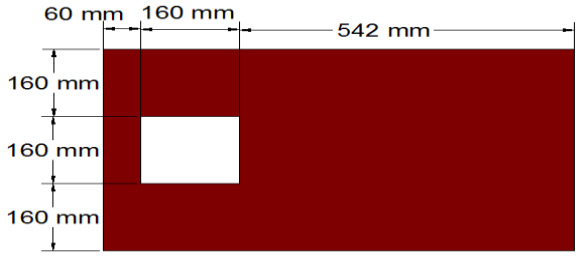

Fig. 6.37 (b) Left center opening in the wall (LCO)

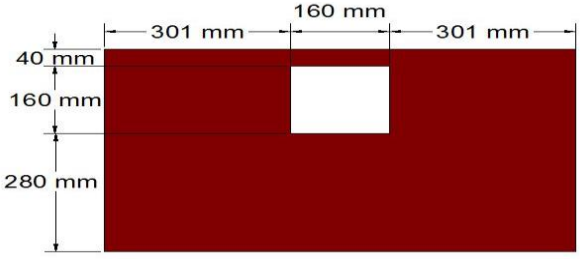

Fig. 6.37 (c) Middle top opening in the wall (MTO)

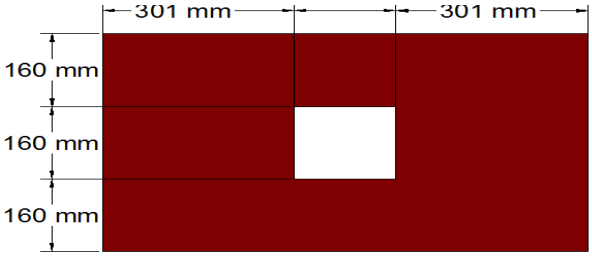

Fig. 6.37 (d) Middle center opening in the wall (MCO)

Fig. 6.37 Flexural strengthened masonry wall with opening at different location

6.4.4.1 Results and discussions of ECC strengthened masonry wall with opening

Table 6.9 depicts the results of parametric study of Serial numbers 10-15 (see Table 6.6) obtained using ABAQUS in terms of normalized flexural strength (M/f_mbd^2) and w_{max}/h. Here, M is the maximum bending moment at the mid-span of the wall; f_m is the masonry compressive strength; b is the width of specimen; d is the distance between the extreme compression fiber of masonry to the centroid of ECC sheet; w_{max} is the maximum mid-span deflection of the specimen; and h is the total depth of the strengthened specimens.

The effect of ECC reinforcement ratio for a fixed value of span, opening, and depth of masonry on the out-of-plane response of strengthened masonry walls with opening is shown in Fig. 6.38. In the graph legend, 'FWOT-10 (4.15%)', the FWOT-10 stands for flexural strengthened masonry wall with 10 mm thick ECC sheet with opening; value in parentheses represents ECC reinforcement ratio which is calculated by cross-sectional area of ECC over total cross-sectional area of strengthened masonry wall. It may be noted that graph is plotted between normalized flexural strength (M/f_mbd^2) and w_{max}/h to propose the design chart of ECC strengthened masonry walls. It is observed that the value of M/f_mbd^2 of strengthened masonry walls with opening (Fig. 6.38) increases with increase in the ECC reinforcement ratio, but with decreased value of w_{max}/h. However, it may be noted that for ECC reinforcement ratio of 9.77%, there is remarkable increase in load carrying capacity as well as deformation capacity. Thus it could be recommended that ECC reinforcement ratio of 9.77% is beneficial for flexural strength of wall with opening. In order to examine the effect of L/d ratio while keeping the width and thickness of the specimens and ECC reinforcement ratio (9.77 %) constant, the length of the specimens was changed from 762 mm to 1500 mm. It is observed from Fig. 6.39 that increase in the L/d ratio (i.e., 2.72 to 5.75) while keeping the constant opening and ECC reinforcement ratio has significantly decreased the normalized flexural strength (M/f_mbd^2) similar to ECC strengthened masonry wall without opening. The w_{max}/h value has increased with increases of L/d ratio for a fixed value of flexural load. It is worth noting that for the lowest value of L/d ratio i.e., (L/d=2.72), the flexural stiffness is higher for the w_{max}/h value up to 0.015 and then drops to that for L/d = 5.75. This shows that for L/d=2.72, shear deformation becomes predominant and reduces the flexural strength.

Figure 6.40 shows the effect of width to thickness ratio (b/h) on the flexural response of the wall with opening. It is observed that for the lowest value of b/h (i.e., b/h=1.88), the normalized flexural

strength ($M/f_m bd^2$) is the highest with the maximum deflection (i.e., w_{max}/h). Thus it could be recommended that b/h=1.88 is beneficial for flexural strength of wall with opening.

The effect of square opening ratio for a fixed size of masonry wall on the out-of-plane response of strengthened masonry walls with opening is shown in Fig. 6.41. In the graph legend, 'SOC (100 × 100), 2.73%', the SOC (100 × 100) stands for square opening of size 100 × 100 mm; values after parentheses represent opening ratio (OR) which is calculated by opening area over total area of strengthened masonry wall. It is observed (Fig. 6.41) that the normalized flexural strength ($M/f_m bd^2$) decreases with increase in opening ratio. However, the impact of opening percentage up to 7% in the case of square opening is not much on the flexural strength. Similar response is observed for rectangular opening ratio of the ECC strengthened wall that the normalized flexural strength ($M/f_m bd^2$) decreases with increase in opening ratio as shown in Fig. 6.42. However, it may be noted that for opening ratios of 3.44% and 6.89%, there is no much difference in the normalized flexural strengths of the walls. Thus it could be recommended that the rectangular opening ratio up to 6.89% is decent without reducing the flexural strength.

Figure 6.43 shows the effect of opening locations on the strengthened masonry walls. The opening locations of strengthened masonry wall have significant effect on the normalized flexural strength. When the opening is considered towards the left top (LTO) & left center (LCO) of the masonry wall a notable decrease in strength as well as displacement is observed as compared with middle central opening (MTO) case and middle top (MTO) case. Hence, the location of opening at the middle center is recommended location for the opening of ECC strengthened masonry walls.

Table 6.9 Results of parametric study of walls with Serial numbers 10-15*

Sr. No.*	Wall designation	Normalized flexural strength $\left(\frac{M}{f_m bd^2}\right)$	$\frac{W_{max}}{h}$
10.	FWOT-10	0.044	0.021
	FWOT-25	0.063	0.031
	FWOT-50	0.069	0.022
	FWOT-75	0.063	0.013
	FWOT-100	0.061	0.009
	FWOT-150	0.065	0.006
11.	FWOL-762	0.063	0.031
	FWOL-1000	0.067	0.033
	FWOL-1250	0.061	0.035
	FWOL-1500	0.058	0.038
12.	FWOW-480	0.063	0.031
	FWOW-750	0.060	0.027
	FWOW-1000	0.061	0.021
13.	SOC (100 × 100)	0.066	0.031
	SOC (160 × 160)	0.062	0.028
	SOC (200 × 200)	0.059	0.026
	SOC (252 × 252)	0.051	0.022
14.	ROC (252 × 50)	0.062	0.036
	ROC (252 × 100)	0.061	0.034
	ROC (252 × 200)	0.059	0.027
	ROC (252 × 300)	0.044	0.020
15.	LTO (160 × 160)	0.036	0.017
	LCO (160 × 160)	0.042	0.023
	MTO (160 × 160)	0.058	0.024
	MCO (160 × 160)	0.062	0.028

* Serial numbers as per Table 6.6.

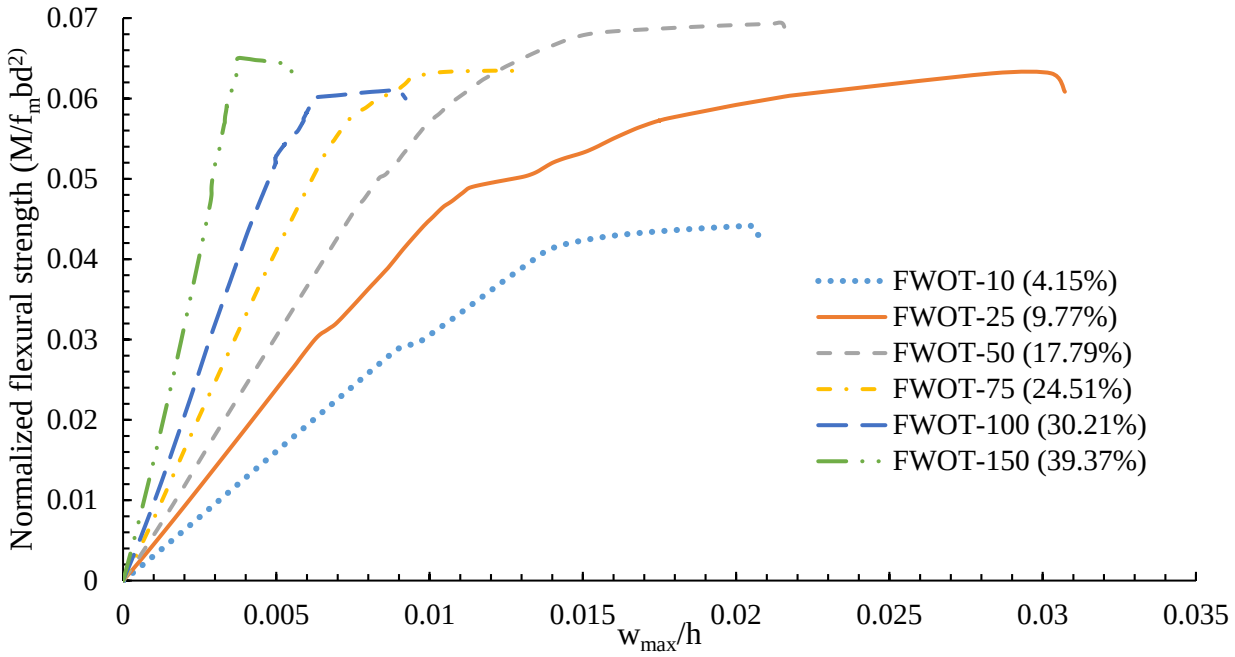

Fig. 6.38 Effect of ECC reinforcement ratio on flexural response of strengthened masonry wall with opening of 11.02%

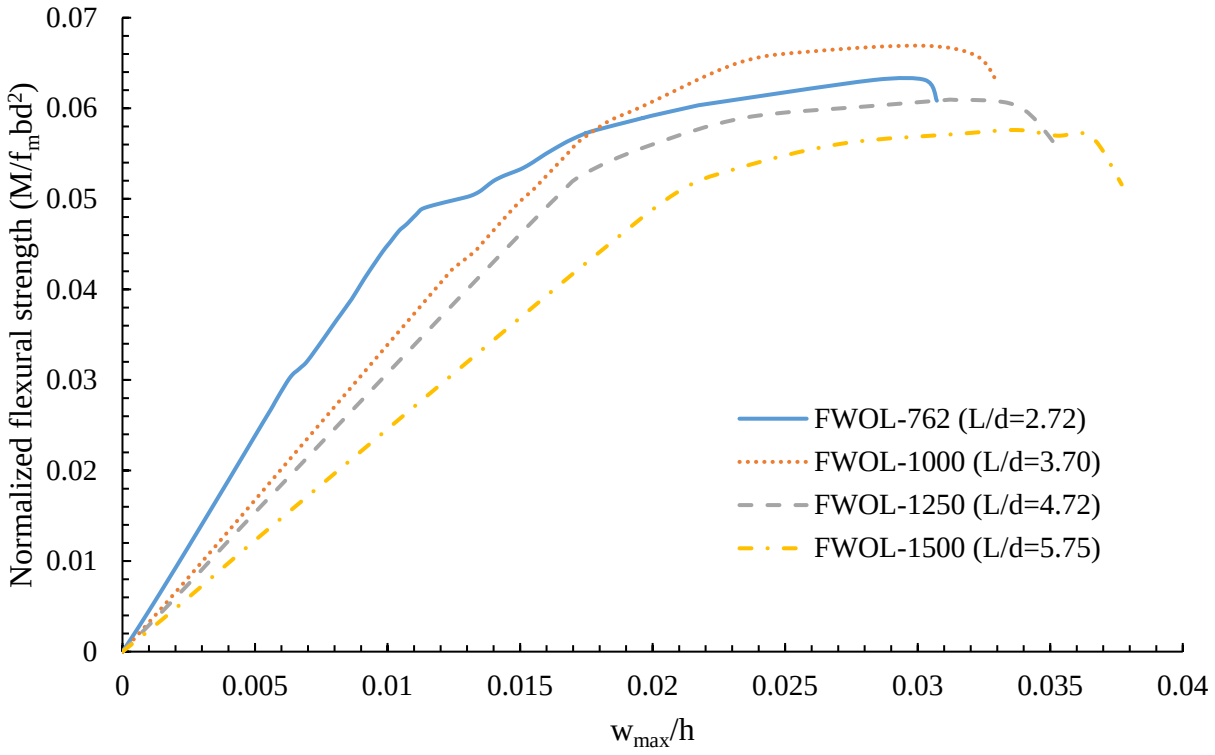

Fig. 6.39 Effect of L/d ratio on flexural response of strengthened masonry wall with opening for ECC reinforcement ratio of 9.77%

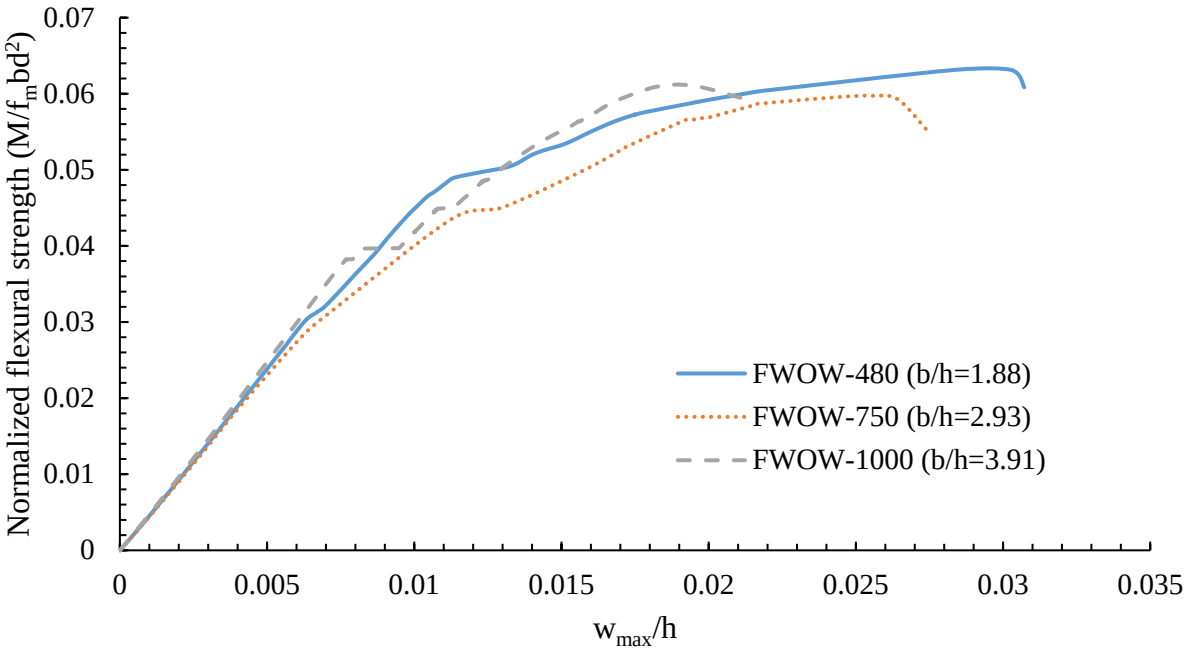

Fig. 6.40 Effect of b/h ratio on flexural response of strengthened masonry wall with opening for ECC reinforcement ratio of 9.77%

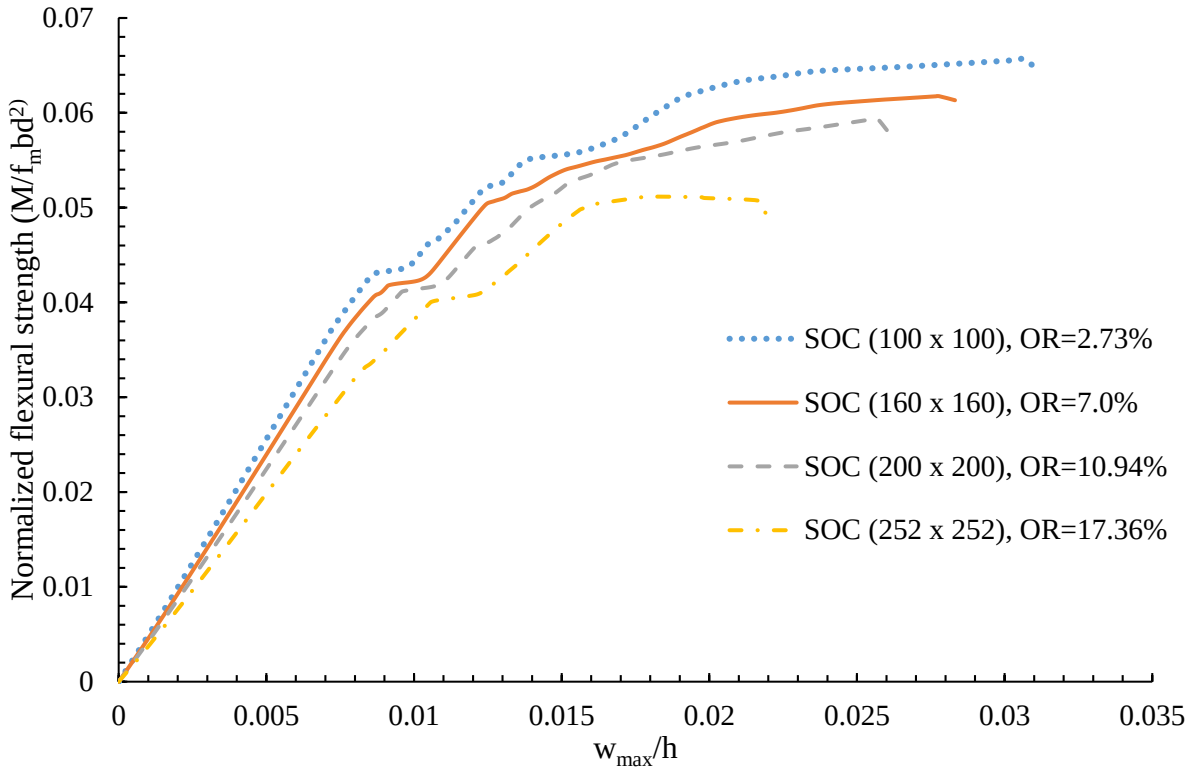

Fig. 6.41 Effect of opening ratio (OR) on flexural response of strengthened masonry wall with square opening

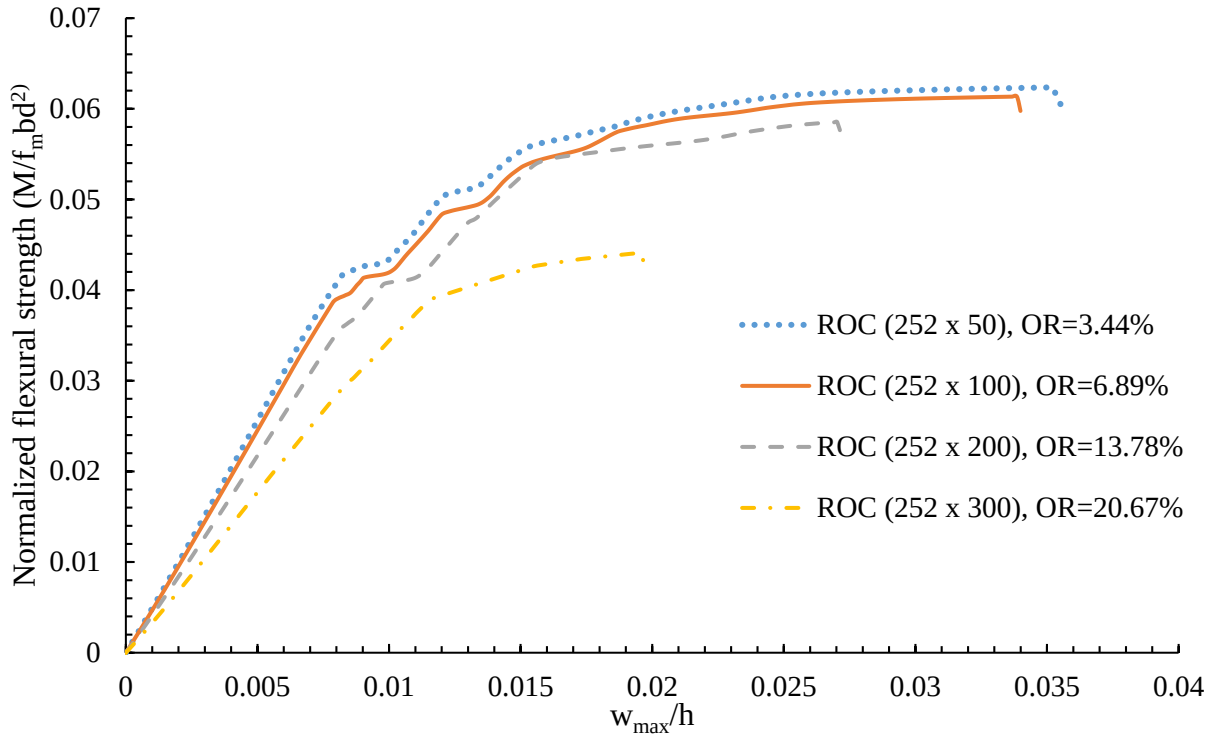

Fig. 6.42 Effect of opening ratio (OR) on flexural response of strengthened masonry wall with rectangular opening

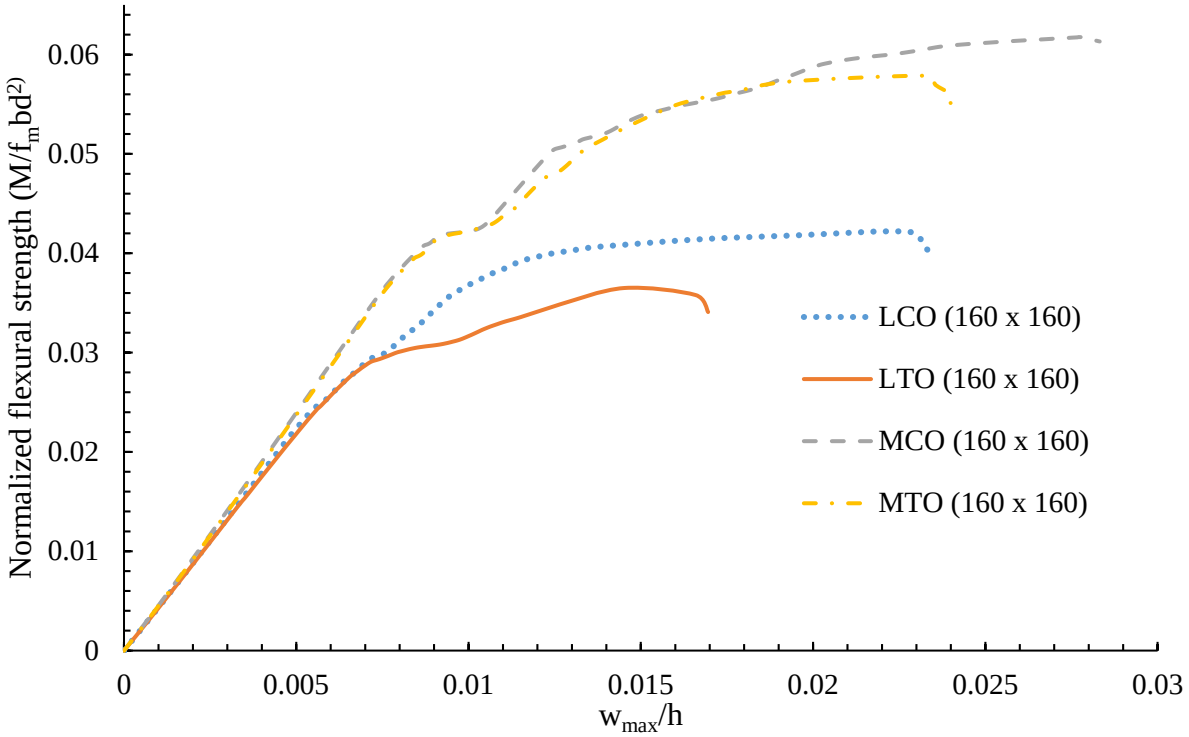

Fig. 6.43 Effect of opening location on flexural response of strengthened masonry wall with opening of size 160 × 160 mm

6.5 Concluding Remarks

The study presents an investigation into the numerical analysis of masonry beams and walls strengthened with ECC sheet in flexure and subjected to out-of-plane loading. The numerical results are validated with corresponding experimental results. A detailed parametric study is also presented to examine the effect of various parameters through numerical modelling using ABAQUS. The following concluding remarks are made regarding the strengthening of masonry beams and walls with ECC sheet and subjected to out-of-plane loading.

- The thickness of epoxy as well as cement mortar significantly influences the flexural response of sandwich beams especially the flexural stiffness, load capacity, and deformability. The smaller thickness results in better flexural response of sandwich beams.
- For tension strengthened beams, the recommended thicknesses of ECC strips are 45 and 50 mm for epoxy and cement mortar as bonding agents, respectively.
- For sandwich beams, the recommended thicknesses of ECC strips for tension and compression faces with epoxy as bonding agent are 45 and 20 mm, respectively.
- Optimum thickness of epoxy bonding agent is 0.5 mm while the recommended thickness range of epoxy bonding agent for ECC strengthened masonry beams is 0.5 to 1.0 mm.
- Optimum thickness of cement mortar is 2 mm while recommended range of cement mortar thickness for ECC strengthened masonry beams is 2 to 4 mm.
- Load carrying capacity of flexural strengthened masonry walls with precast ECC sheet is found to be about 5 times of that of control/unstrengthened masonry walls.
- The numerical results are sensitive to the mesh element size of the concrete damage plasticity (CDP) model. Accurate element mesh size of CDP model is essential for the finite element analysis.
- A design chart for ECC strengthened masonry walls is presented for a limited range of geometrical parameter expressed as non-dimensional parameter.
- These design charts will help the designer to determine the necessary ECC reinforcement ratio as per required strength in the strengthened masonry walls.
- It is recommended that for a given span to depth ratio, width to thickness ratio of 3.91 is beneficial, while the span to depth ratio should be equal or greater than 3.70 to avoid the

negative effect of shear deformations in the case of ECC strengthened masonry wall without opening.

- It is observed that the normalized flexural strength ($M/f_m bd^2$) decreases with increase in opening ratio of ECC strengthened masonry wall with opening. However, for square opening, impact of opening percentage up to 7% is considerably low on its flexural strength.
- The location of opening plays the crucial role on the flexural response of ECC strengthened masonry wall with opening. When the opening is considered towards left top & left center of the masonry wall a notable decrease in strength as well as displacement is observed as compared with central opening case.
- It is recommended that the rectangular and square opening ratio up to 7% is decent without significantly compromising the flexural strength.